Res Chem Intermed
DOI 10.1007/s11164-012-0783-7

Application of photo catalysis for mitigation of carbon dioxide

V. Jeyalakshmi · K. Rajalakshmi · R. Mahalakshmy · K. R. Krishnamurthy · B. Viswanathan

Received: 8 April 2012 / Accepted: 18 August 2012

Abstract Photo catalytic reduction of carbon dioxide by water or *artificial photosynthesis* to yield hydrocarbons (methane and methanol, etc., termed "solar fuels") is being studied extensively, with the twin objectives of developing an effective means of limiting atmospheric CO_2 levels and evolving a sustainable alternative route for production of fuels and chemicals. This short review covers the origin and thermodynamic and kinetic features of the process, the basic photocatalytic principles involved, the rationale behind the choice of different catalysts and their performance, the effect of process conditions, the effect of the structural and photophysical properties of the different catalysts on their performance, mechanistic pathways, surface transformations, challenges involved in the practical application of the process, and future directions for research.

Keywords Photo catalysis · photo catalytic reduction · CO_2 mitigation · Structure–photophysical properties–performance relationships

V. Jeyalakshmi · K. Rajalakshmi · K. R. Krishnamurthy · B. Viswanathan (✉)
National Centre for Catalysis Research, Indian Institute of Technology, Madras, Chennai 600036, Tamilnadu, India
e-mail: bvnathan@iitm.ac.in

V. Jeyalakshmi
e-mail: vmjeya@gmail.com

K. Rajalakshmi
e-mail: raji2807@gmail.com

K. R. Krishnamurthy
e-mail: krkm@iitm.ac.in

V. Jeyalakshmi · R. Mahalakshmy
Department of Chemistry, Thiagarajar College, Madurai Kamaraj University, Madurai 625021, Tamilnadu, India
e-mail: mahabioin@yahoo.com

Journal : Small-ext 11164 | Dispatch : 26-10-2012 | Pages : 38
Article No. : 783 | LE | TYPESET
MS Code : | CP | DISK

Heterogeneous photocatalysis

The consistent study of photo catalytic reactions was initiated in 1970s. The concept and the term "heterogeneous photocatalysis" were introduced and developed in Lyon to describe the partial oxidation of alkanes and olefinic hydrocarbons. Heterogeneous photocatalysis is defined as "a catalytic process during which one or more reaction steps occur by means of electron–hole pairs photogenerated on the surface of semiconducting materials illuminated by light of suitable energy" [1]. This pathway differs from the usual thermal reaction sequence and leads to reaction product selectivity patterns different from those of thermal or catalyzed reactions.

Principles and elementary steps

The electronic structure of bulk solids is best described by the classical band theory of solids. The two outermost energy levels, called as valence band (VB) and conduction band (CB), are responsible for solid-state properties, conductivity, and reactivity. The highest energy band, in which all energy levels are occupied by electrons, is called the VB, whereas the CB is the lowest energy band without electrons. The energy interval (ΔE_g) between the VB and CB is the "band gap", which is the characteristic for the electronic structure of a semiconductor. According to the band gap model (Scheme 1) for photocatalysis proposed by Demeestere et al. [2], VB electrons are transferred to the CB when the semiconductor is illuminated with photons of energy equal to or higher than the band gap, creating electron–hole pairs (1). After migration to the semiconductor surface (2), electron–hole pairs may participate in redox reactions with adsorbed surface species having suitable redox potentials (3). Thermodynamically, VB holes can oxidize adsorbed species if the redox potential of the VB is more positive than that of the adsorbed species. Similarly, CB electrons can reduce adsorbed species if they have a higher negative redox potential than that of adsorbed species. In the absence of such reactions with the surface species, electron–hole pair recombination occurs with release of thermal energy and/or light (4).

The rate of a photo catalytic reaction especially depends on the type of photo catalytic semiconductor and on the light radiation used in for initiation [3]. Other factors that affect a photo catalytic reaction are:

- the pH of the medium with which the semiconductor surface is in contact;
- the concentration of the substrate affecting the reaction kinetics;
- the stream of photons, because oversupply of light accelerates electron–hole recombination; and
- the temperature, because higher temperatures cause frequent collisions between semiconductor and substrate.

Applications of photocatalysis

A variety of applications, ranging from anti-fogging, anti-microbe, and self-cleaning surfaces, to water and air purification and solar induced hydrogen

Journal : Small-ext 11164 | Dispatch : 26-10-2012 | Pages : 38
Article No. : 783 | LE | TYPESET
MS Code : | CP | DISK

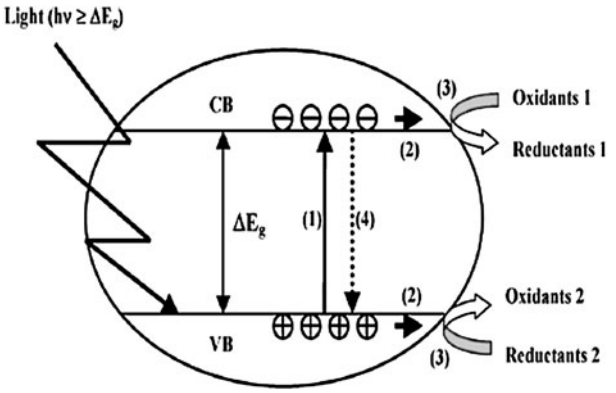

Scheme 1 Schematic representation of the "band gap model" (*1*) photo-induced electron–hole pair creation; (*2*) charge migration to the surface; (*3*) redox reactions; (*4*) recombination. *VB* and *CB* represent the valence band and conduction band, respectively (reproduced from Ref. [2], with permission from Taylor and Francis; copyright 2007)

production, have been developed, and many of these have been used in commercial products. However, extensive research continues to further optimize this technology and to widen the range of potential applications, especially in the following areas:

- *Conversion of water into hydrogen gas by photo catalytic water splitting.* The ultimate target of water splitting is to provide clean H_2 fuel by utilization of solar energy. Extremely efficient solar splitting of water has been reported for the photovoltaic–photoelectrolytic device of Khaselev and Turner and for the photovoltaic–electrolytic device of Licht [4].
- *Conversion of carbon dioxide into hydrocarbons by use of water.* In this case, photocatalysis provides a way of mimicking photosynthesis by using a semiconductor catalyst to absorb and utilize solar energy to convert CO_2 into fuels and chemicals.
- Application of illuminated semiconductors for *remediation of contaminants* has been used successfully for a wide variety of compounds, for example alkanes, aliphatic alcohols, aliphatic carboxylic acids, alkenes, phenols, aromatic carboxylic acids, and dyes, polychlorinated biphenyls, simple aromatic compounds, halogenated alkanes and alkenes, surfactants, and pesticides, and for reductive deposition of heavy metals (e.g., Pt^{4+}, Au^{3+}, Rh^{3+}, $Cr^{(VI)}$) from aqueous solution on to surfaces [5].
- Use of titanium dioxide in *self-cleaning glass*. Free radicals generated from TiO_2 oxidize organic matter. photo catalytic surfaces have the potential to act against a variety of air pollutants and odors, for example microbes, volatile organic compounds (VOCs), formaldehyde, ammonia, and inorganic gaseous substances, for example oxides of nitrogen or sulfur (NO_X, SO_X).
- *Disinfection of water* by titanium dioxide photocatalysis.

Journal : Small-ext 11164 | Dispatch : 26-10-2012 | Pages : 38
Article No. : 783 | LE | TYPESET
MS Code : | CP | DISK

Components used with the photocatalyst

In addition to the photocatalyst, whose primary function is to absorb light energy, several other components can, depending on the application, be added to modify the photocatalyst system and improve overall efficiency [6].

photo catalytic systems based on semiconductors and sensitizers

The large group of the light-sensitive materials that have been investigated as photocatalysts includes fairly wide-band semiconductors, mostly metal oxides that absorb UV light. One method of extending their light sensitivity to the visible region of the spectrum is to use colored substances and/or dyes or sensitizers (Scheme 2).

Sensitization by light harvesting dyes and macrocyclic ligands, for example phthalocyanins (Pcs) and porphyrins (Prs), involves transfer of photogenerated electrons directly into the CB of the semiconductor, TiO_2 in this example [7, 8]. Such macrocyclic ligands are good candidates for sensitization because of their high absorption coefficient in the visible region of the solar spectrum and good chemical stability. Because photoelectrons are directly transferred to the CB of titania, charge-carrier separation is very effective. Pr–titania composites have excellent activity in photo-catalytic degradation of rhodamine-B by visible light and titania containing Fe–Pr is active in the UV range [9, 10]. Zhihuan et al. [11] and Shaohua et al. [12]. observed that Pcs containing Zn and Co prepared by the sol–gel technique were active in photo catalytic reduction of CO_2. A few more examples are described in the section "Titania dispersed on different meso/nano porous and macrocyclic matrices".

photo catalytic systems based on semiconductor hetero structures

In binary systems based on narrow-band and wide-band semiconductors, absorption of visible light by the narrow-band component leads to the injection of an electron into the wide-band semiconductor. The hole remains spatially separated from the electron and interacts with the electron donor (Scheme 3).

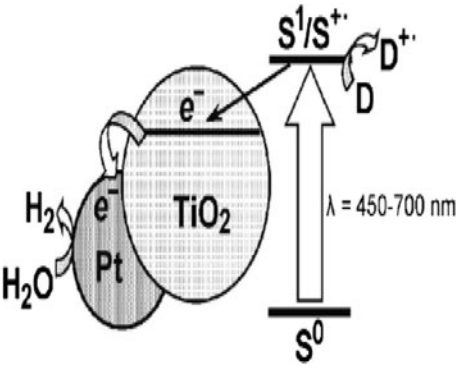

Scheme 2 Operation of a photo catalytic system based on metal–semiconductor structures and a dye-sensitizer for release of hydrogen from water. *S0*, *S1*, and *S+* are the sensitizer in the ground, excited, and one-electron oxidized states of the dye, respectively (reproduced from Ref. [6], with permission from Springer Science and Business Media; copyright 2009)

Journal : Small-ext 11164 | Dispatch : 26-10-2012 | Pages : 38
Article No. : 783 | LE | TYPESET
MS Code : | CP | DISK

An elegant example of hetero-structured semiconductors or coupled semiconductors is the Cu_2O–TiO_2 system (Fig. 1) developed by Huang et al. [13]. Cu_2O, with a band gap of 2.0 eV, is a typical narrow-band semiconductor with both CBs and VBs located above those of TiO_2, a state which thermodynamically favours transfer of excited electrons and holes between them. This state of energy levels facilitates all four charge-transfer processes indicated in Fig. 1, in the UV and visible regions. Whereas processes 1 and 2 can proceed with UV and visible radiation, processes 3 and 4 require UV radiation. All four processes together constitute a highly effective coupled semiconductor system, with very high efficiency. Hetero structures with 30 and 70 % Cu_2O, both under UV and visible irradiation, are 6 and 27 times more active, respectively, than the base material, P25 [13].

Examples are known wherein narrow-band semiconductors, for example PbS, CdS, and CdSe, are used to form effective hetero structures with TiO_2 [14–16]. Inherent drawbacks with such systems are photo-corrosion and charge–carrier recombination. In such cases electron donors, for example sulfide or sulfite, are added as hole scavengers.

Photocatalyst systems based on semiconductors doped with metal cations

The doping of wide-band semiconductors with transition metals creates local states in the forbidden band. Excitation of electrons from those local states by visible light leads to transfer of electrons into the CB (Scheme 4).

Doped metals act as electron traps, facilitating charge separation and preventing recombination. Experimental evidence of this effect was presented by Anpo and Takeuchi [19] in their studies on Pt loaded on TiO_2. As shown in Fig. 2, pure titania, when irradiated with UV light, gives ESR signals attributed to Ti^{3+} formed by the photogenerated electrons. On loading the TiO_2 with Pt, the intensity of the ESR signal from Ti^{3+} falls sharply, because of transfer of electrons from titania to Pt. The holes remain in the TiO_2, resulting in charge separation.

The effect of metal ion doping on the characteristics of titania, and improvements observed in photo catalytic activity for a variety of reactions have been studied extensively [17–27]. A comprehensive study on the effects of the doping of 21

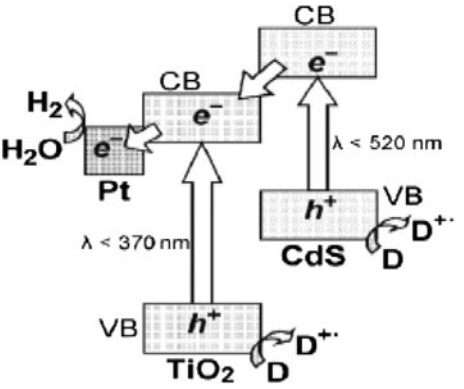

Scheme 3 Spatial separation of the photogenerated charges in the CdS/TiO_2 hetero-structure and the formation of hydrogen during the action of visible light (reproduced from Ref. [6], with permission from Springer Science and Business Media; copyright 2009)

Journal : Small-ext 11164 | Dispatch : 26-10-2012 | Pages : 38
Article No. : 783 | LE | TYPESET
MS Code : | CP | DISK

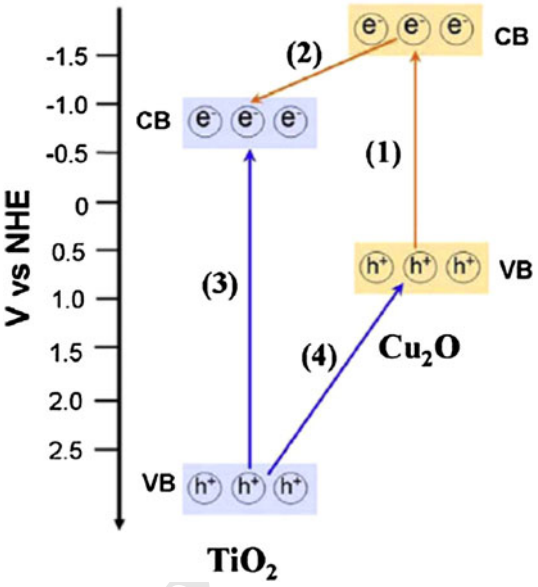

Fig. 1 Photo-generation and separation of charge carriers in Cu_2O–TiO_2 hetero-structure in the UV and visible regions (reproduced from Ref. [13], with permission from Elsevier; copyright 2009)

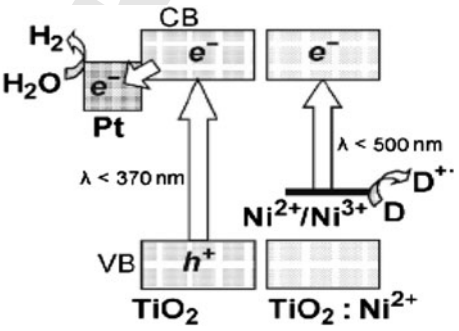

Scheme 4 Operation of the photo catalytic system for the release of hydrogen from an aqueous solution of electron donor D with participation of titanium dioxide doped with Ni^{2+} (TiO_2:Ni^{2+}) (reproduced from Ref. [6], with permission from Springer Science and Business Media; copyright 2009)

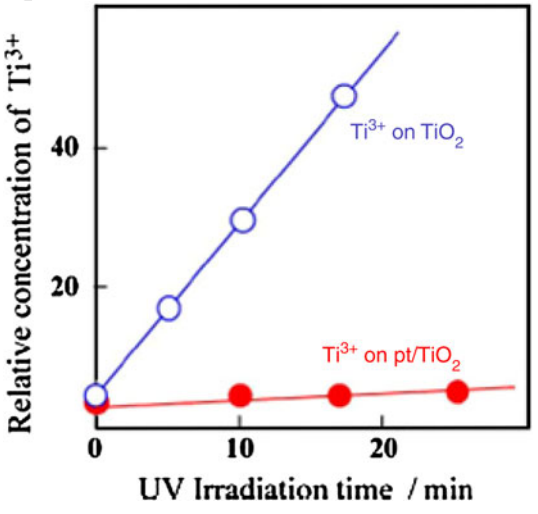

Fig. 2 Growth of ESR signal intensity (at 77 K) of the photo-formed Ti^{3+} active site on Pt-loaded and unloaded TiO_2 (reproduced from Ref. [19], with permission from Elsevier; copyright 2003)

Journal : Small-ext 11164 | Dispatch : 26-10-2012 | Pages : 38
Article No. : 783 | LE | TYPESET
MS Code : | CP | DISK

metal ions on titania has been reported by Choi et al. [23]. who observed that doping significantly affects photo-reactivity in the degradation of $CHCl_3$, charge carrier recombination rates, and interfacial electron-transfer rates. Doping titania with Fe^{3+}, Mo^{5+}, Ru^{3+}, Os^{3+}, Re^{5+}, V^{4+}, and Rh^{3+} at 0.1–0.5 at.% significantly increases photo catalytic activity in both oxidation and reduction reactions whereas doping with Co^{3+} and Al^{3+} reduces activity. Photo-reactivity increases with the relative concentration of trapped charge carriers and seems to be a complex function of the dopant concentration, the energy level of dopants within the TiO_2 lattice, their "d" electronic configuration, the distribution of dopants, the electron donor concentration, and the intensity of the light.

Photocatalyst systems based on semiconductors doped with anions

One approach to narrowing of the forbidden band in oxide semiconductors is partial substitution of the oxygen by other elements (nitrogen, carbon, and sulfur), which makes it possible to realize "band design", i.e., intentional shift of the VB of the photocatalyst by virtue of the fact that the p orbitals of the impurity are situated in the VB above the p orbitals of the oxygen, thereby narrowing the forbidden band without substantially moving the bottom of the CB (Scheme 5).

Introduction of anions of N and S into TiO_2 results in narrowing of the band gap because of mixing of the p states of dopants (N, S) with oxygen 2p states in the valance band of TiO_2 and creation of impurity states above the VB of titania [7, 8]. Such changes in the electronic structure of TiO_2 facilitate visible light absorption. Although several anions of C, N, F, P, and S have been used for doping titania, studies on doping with nitrogen has been predominant [17–22]. According to Asahi et al. [28, 29] substitutional doping is possible by mixing the 2p states of oxygen from titania with the 2p states of N, resulting in intra-band states which, in turn, can effectively narrow the band gap, thereby facilitating use of visible light. Interstitial-type doping is found to be ineffective.

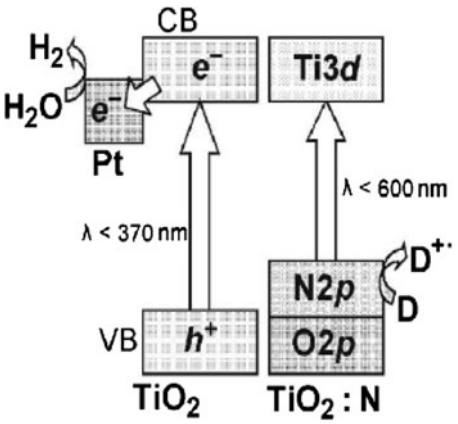

Scheme 5 Operation of the photo catalytic system for release of hydrogen from an aqueous solution of electron donor D with participation of titanium dioxide doped with nitrogen (TiO_2:N) (reproduced from Ref. [6], with permission from Springer Science and Business Media; copyright 2009)

Journal : Small-ext 11164 | Dispatch : 26-10-2012 | Pages : 38
Article No. : 783 | LE | TYPESET
MS Code : | CP | DISK

In contrast, Valentin et al. [30, 31] propose absorption of nitrogen in the substitutional state as more effective in the formation of localized levels within the band gap and conclude that both substitutional and interstitial nitrogen may exist with energy levels as shown in Fig. 3, depending on the preparation conditions. Two N 1s XPS peaks observed for N-doped titania, one at 396 eV for substitutional nitrogen species and the other at 400 eV for interstitial nitrogen species lend credence to this theory [18]. Although assignment of the XPS peak at 396 eV for substitutional N species has been corroborated by other researchers [32–34] there is raging controversy over the proposed peak from interstitial N species at 400 eV, which has been attributed to different species, for example N–O–Ti–O or O–N–Ti–O [35, 36].

The main features of these modifications and implications for the properties of titania, applicable in any typical semiconductor, are summarized in Table 1.

Mitigation of carbon dioxide

CO_2—the greenhouse gas

CO_2 occurs in nature and serves as source of carbon for photosynthesis of plants and crops. It is present in the atmosphere with a volumetric concentration of 0.039 % (389 parts per million by volume, ppmv). Emission of carbon dioxide into the atmosphere, released mainly during burning of fossil fuels, is one of the most serious problems with regard to the greenhouse effect. All human activity generates approximately 37 billion tons (37 Gt) of CO_2 emissions each year, with approximately 30 Gt of this coming from energy-related emissions.

Total emissions were less than 25 Gt 20 years ago. In the current scenario, emissions are projected to rise to over 50 Gt 20 years from now. Burning 1 t of carbon in fossil fuels releases more than 3.5 t of carbon dioxide [37]. The Earth's surface temperature has risen by approximately 0.6 K in the past century, with particularly significant warming trends and changes in weather conditions over the

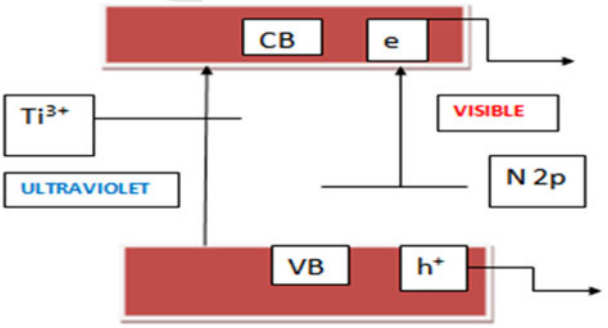

Fig. 3 Schematic energy level diagram for nitrogen-substituted TiO_2 (the bare semiconductor absorbs UV radiation and localized energy levels of nitrogen above the VB facilitate absorption of visible light) (reproduced from Ref. [30], a Hindawi Publishing Corporation-open journal)

Journal : Small-ext 11164 | Dispatch : 26-10-2012 | Pages : 38
Article No. : 783 | LE | TYPESET
MS Code : | CP | DISK

Table 1 Implications of different modifications in titania

Modification	Implications and/or mode of action
Doping with metals/metal ions	Act as electron traps and facilitate charge-carrier separation
	Introduce impurity states and induce visible light absorption
	Absorb visible light via surface plasmon resonance
Doping with anions	Narrowing of band gap because of mixing of p states of dopants (N, S) with O 2p states in the valance band of TiO_2
	Introduce impurity states above the VB of titania
	Both states induce visible light absorption
Coupling with semiconductors	A narrow band gap semiconductor, with appropriate energy levels, absorbs visible light and transfers excited electrons into the CB of titania. UV light source not needed
	Besides visible light activity, effective separation of charge carriers is achieved
Sensitization with light harvesting components and/or dyes	Light-absorbing components can absorb visible light and inject photo-excited electrons into the CB of titania
	Besides visible light activity, effective separation of charge carriers is achieved

past two decades. Hence CO_2 reduction and management (capture, storage, and sequestration) has become a crucial issue in controlling global warming.

Approaches toward reduction of CO_2 emission

Reduction in CO_2 emissions can be achieved by three different approaches [22]:

1. Efficient use of carbon-based energy sources,
2. Use of alternative or carbon-free energy sources,
3. Use of post-treatment carbon capture technology.

Although efforts on all three approaches are being pursued globally, carbon capture technology is gaining prominence. In carbon capture, CO_2 is removed from industrial flue gas by a gas-separation process before release to the atmosphere. Captured and stored CO_2 could be recycled by conversion into useful chemicals and fuels.

Carbon sequestration

Carbon sequestration (storage) is the isolation of carbon dioxide (CO_2) from the Earth's atmosphere. Sequestration could be highly important in preventing continued CO_2 build up in the atmosphere.

Geological sequestration involves storing CO_2 underground in rock formations that can retain large quantities of CO_2 for long periods of time. The CO_2 would be held in small pore spaces inherent in rocks. It is possible that CO_2 injection into coal seams and mature oil fields could assist in the extraction of coal bed methane or oil

Journal : Small-ext 11164 | Dispatch : 26-10-2012 | Pages : 38
Article No. : 783 | LE | TYPESET
MS Code : | CP | DISK

that would otherwise be left in the ground, which could help offset the costs of sequestration.

Other carbon-capture technology

Currently, technology such as gas absorption by chemical solvents, permeation through membranes, cryogenic distillation, and gas adsorption by solid sorbents are available for the capture of CO_2 from flue gas. However these are not economically feasible [22].

CO_2 conversion

Because CO_2 is the most oxidized form of carbon, only chemical transformation at normal energies could possibly reduce it. A wide range of CO_2 conversion techniques are under investigation [38]; there include:

(i) *Chemical reduction by metals at relatively at high temperatures*

$$2Mg + CO_2 \rightarrow 2MgO + C \quad (1)$$

$$Sn + 2CO_2 \rightarrow SnO_2 + 2CO \quad (2)$$

$$2Na + CO_2 \rightarrow Na_2C_2O_4 \quad (3)$$

(ii) *Thermochemical conversion*

$$CO_2 \xrightarrow{Ce^{4+},\ T\ >\ 900\,^{\circ}C} CO + 1/2O_2 \quad (4)$$

(iii) *Radiochemical method*

$$CO_2 \xrightarrow{\gamma-\text{Radiation}} HCOOH, HCHO \quad (5)$$

(iv) *Photo-chemical conversion*

$$CO_2 \xrightarrow{h\nu} CO, HCHO,\ HCOOH \quad (6)$$

(v) *Biochemical conversion*

$$CO_2 + 4H_2 \xrightarrow{\text{Bacteria}} CH_4 + 2H_2O \quad (7)$$

The bacteria *Methanobacterium thermoautotrophicum* can be immobilized in a fixed bed or on hollow fibers; feeding stoichiometric ratio for the reaction achieves 80 % of the theoretical yield.

(vi) *Electrochemical conversion*

$$CO_2 + xe^- + xH^+ \xrightarrow{eV} CO, HCOOH, (COOH)_2 \quad (8)$$

Journal : Small-ext 11164 | Dispatch : 26-10-2012 | Pages : 38
Article No. : 783 | LE | TYPESET
MS Code : | CP | DISK

(vii) *Biophotochemical conversion*

The "bio" part of the energy consists in the catalysis and information content of an enzyme:

$$CO_2 + \text{oxoglutaric acid} \xrightarrow{h\nu} \text{isocitric acid} \quad (9)$$

(viii) *Electrophotochemical conversion*

$$CO_2 + 2e^- + 2H^+ \xrightarrow{h\nu,\ eV} CO + 2H_2O \quad (10)$$

Conventional catalytic reduction of CO_2 to chemicals (formic acid, methanol, methane, etc.) by use of external hydrogen is feasible [39] but hydrogen has to be produced via renewable resources to render it viable and sustainable.

photo catalytic CO_2 reduction

The challenge

The CO_2 reduction process is thermodynamically uphill, as illustrated by its standard free energy of formation ($\Delta G^\circ = -394.359$ kJ/mol) [40]. Economical CO_2 fixation is possible only if renewable energy, for example solar energy, is used as the energy source. Equally difficult is the reduction and/or splitting of water to yield hydrogen and, hence, requires a similar combination of activation steps. The most ideal and desirable process would then be simultaneous reduction of CO_2 and water to yield hydrocarbons, which is, essentially, artificial photosynthesis.

The utilization of solar energy via chemical storage can be achieved by photo catalytic or photoelectrochemical activation of light-sensitive catalytic surfaces. When the two systems are compared, the photo catalytic system is simpler, and easy to construct and operate. The photo catalytic process occurs via direct absorption of photons with energy greater than or equal to the band gap of the photocatalyst, generating electron–hole pairs. The initial excitation and electron energy transfer to the adsorbed reactants on the photocatalyst make chemical reactions in the photo catalytic process possible.

Thermodynamics

There are two conceptual routes to producing renewable carbon containing fuels by use of solar energy [40]:

- direct photoreduction of CO_2 using water as a reductant; and
- photolysis of water to generate hydrogen and further reaction of this hydrogen with carbon dioxide forming C_1–C_2 fuels.

Journal : Small-ext 11164 | Dispatch : 26-10-2012 | Pages : 38
Article No. : 783 | LE | TYPESET
MS Code : | CP | DISK

The first route, which mimics natural photosynthesis, is the preferred one. Water splitting and carbon dioxide reduction processes take place simultaneously on the photocatalyst/co-catalyst surface, and the thermodynamic requirements of these processes put constraints on the band gap of the materials used as photocatalysts. Hydrogen formation from water involves a free energy change ($\Delta G°$) of 237 kJ/mol and an enthalpy change ($\Delta H°$) of 285 kJ/mol; the corresponding values for CO formation from CO_2 are 257 and 283 kJ/mol at 25 °C (1 atm). Hence, the minimum energy required for water and CO_2 splitting processes are 1.229 and 1.33 eV (per photon) respectively. In theory, the band gap of a photocatalyst used for co-splitting of CO_2 and water should be at least 1.33 eV [40]. One, two, four, six, and eight electron reduction potentials (vs. NHE) for CO_2 reduction and H_2O oxidation at pH 7 and 25 °C, assuming unit activity for all gaseous and aqueous species are given below [40].

Reaction	E^0_{redox} (V vs. NHE)	
$2H^+ + 2e^- \rightarrow H_2$	−0.14	(11)
$H_2O \rightarrow 1/2O_2 + 2H^+ + 2e^-$	−0.82	(12)
$CO_2 + e^- \rightarrow CO_2^-$	−1.9	(13)
$CO_2 + H^+ + 2e^- \rightarrow HCO_2^-$	−0.49	(14)
$CO_2 + 2e^- + 2H^+ \rightarrow CO + H_2O$	−0.53	(15)
$CO_2 + 4H^+ + 4e^- \rightarrow HCHO + H_2O$	−0.48	(16)
$CO_2 + 6H^+ + 6e^- \rightarrow CH_3OH + H_2O$	−0.38	(17)
$CO_2 + 8H^+ + 4e^- \rightarrow CH_4 + 2H_2O$	−0.24	(18)

From these equations it is clear CO_2 photoreduction is not a single-step reaction. Upon transfer of one electron, the structure changes from the linear to bent configuration, which results in irreversible reduction [38]. Single electron transfer to CO_2 is also highly endergonic, because of the negative adiabatic electron affinity of CO_2.

The initial step in the photo catalytic reduction of CO_2 is the generation of electron–hole pairs upon absorption of photons of energy greater than or equal to the band gap of the photocatalyst. The time scale of this electron–hole recombination is two to three orders of magnitude faster than other electron-transfer processes. Therefore, any process which inhibits electron–hole recombination would greatly increase the efficiency and improve the rates of CO_2 photoreduction. The kinetics of CO_2 photoreduction also depend upon many other factors, for example incident light intensity, fraction of the incident light absorbed by the photocatalyst, specific surface area of the photocatalyst absorbing the light, etc.

Choice of catalysts—guiding principles

It is essential that the photogenerated electrons should have the requisite energy, as indicated by thermodynamic criteria, to facilitate the reduction of CO_2. This means

Journal : Small-ext 11164 | Dispatch : 26-10-2012 | Pages : 38
Article No. : 783 | LE | TYPESET
MS Code : | CP | DISK

that the CB bottom energy level of the photocatalyst has to be more negative than the energy for CO_2 reduction and the VB top energy level has to be more positive than the energy for oxidation of water. Thus, the choice of catalyst for CO_2 photoreduction with water is determined by the relationship between the energy levels of the CBs and VBs vis-a-vis the energies for CO_2 reduction and water oxidation. Pioneering studies on photoelectrocatalytic reduction of CO_2 on a variety of semiconducting oxides has revealed the basic criteria for catalytic activity. This guiding principle was illustrated effectively by Inoue et al. [41] for the relationship between the energy levels of CBs and VBs and the those of the redox couples, as depicted in Fig. 4.

Semiconductors, for example SiC, GaP, CdS, ZnO, and TiO_2, which satisfy the above criteria are active in photoreduction of CO_2 whereas oxides, for example WO_3 and SnO_2, whose CB levels are below that for CO_2 reduction, have failed to perform. Energy levels of CB and VB versus those for redox couple and the lifetime of charge carriers, prolonged by reduced rates of recombination, are the two fundamental criteria to be considered for selection of the catalyst for CO_2 photoreduction.

Wide band-gap semiconductors are the most suitable photocatalysts for CO_2 reduction, because they provide sufficient negative and positive redox potentials in the CBs and VBs, respectively. The disadvantage of using wide band-gap semiconductors is the requirement for high energy input.

Although many semiconductors have smaller band gaps and absorb in the visible range (e.g. CdS and Fe_2O_3 with band gaps of 2.4 and 2.3 eV, respectively), only a few are catalytically active, because the energy levels of either the CBs or VBs are unsuitable for CO_2 reduction and/or water oxidation (Fig. 4). This limitation, with poor photo-corrosion stability of many semiconductors, significantly limits the number of potential photo catalytic materials for CO_2 photoreduction.

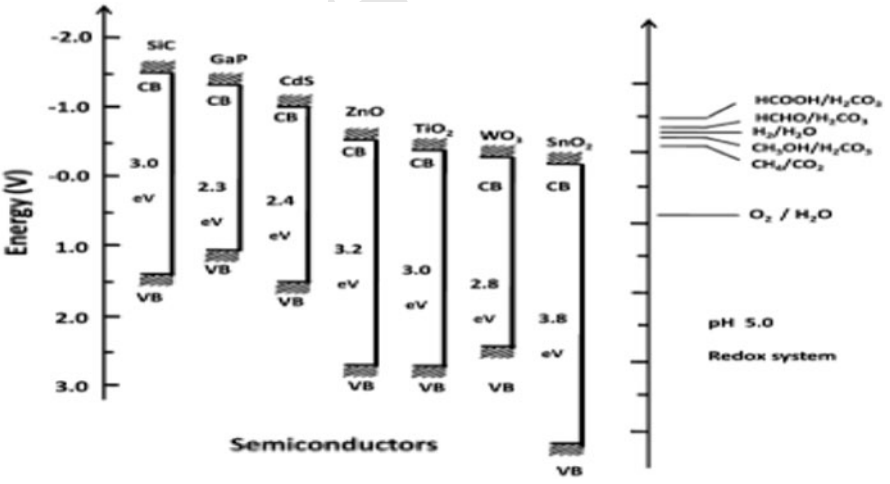

Fig. 4 CB and VB potentials of semiconductor photocatalysts relative to energy levels of the redox couples in water (reproduced from Ref. [40], with permission from Macmillan; copyright 1979)

Journal : Small-ext 11164 | Dispatch : 26-10-2012 | Pages : 38
Article No. : 783 | LE | TYPESET
MS Code : | CP | DISK

CO_2 photoreduction: effect of process conditions

Effect of wavelength and light intensity

Semiconductors absorb light radiation with the threshold wavelength that provides sufficient photon energy to overcome the band gap between the VBs and CBs. This threshold wavelength, required to promote the excited state, corresponds to the minimum photon energy and depends on the band gap energy; for example, for TiO_2 anatase with band gap energy 3.2 eV it is 387.5 nm [2].

Irradiation using light of shorter wavelength (254 nm) is significantly more effective for CO_2 reduction using TiO_2 than that with a longer wavelength (350 nm) [42]. The wavelength (λ) of the light used affects the yield of products, as observed by Fan et al. [43] in their studies on N (4 % *w*/*w*) and Ni (6 % *w*/*w*) co-doped titania for CO_2 reduction with water. For this catalyst formulation, Fan et al. [43] observed methanol yields of 482, 253.5, and 120.5 (all in μmol/g cat) for radiation of wavelength 254, 365, and 400–780 nm respectively, clearly indicative of the effect of the wavelength of the light used.

Electrons in excited states are produced via electronic transitions, the probability of which depends on the intensity of the light. At low light intensities, the rate of CO_2 reduction increases linearly with light intensity. At mid-range light intensities the photo catalytic reaction rate is dependent on the square root of light intensity, and at high light intensities the rate is independent of light intensity [2].

Variations in the wavelength of the radiation used can also affect the rate of formation of products, as observed by Liu et al. [44] with $BiVO_4$ catalysts (Table 2). Monoclinic $BiVO_4$ was found to be more active than the tetragonal form. Selective formation of ethanol is observed when 300-W UV radiation is used, with and without a UV cut-off filter. With a 36-W lamp, however, both alcohols are formed at nearly same rate, although overall conversion is much less.

Effect of reaction pressure

Mizuno et al. [45] observed that CO_2 photoreduction with water containing dispersed TiO_2 increased with increasing CO_2 pressure. Increasing solubility of CO_2 in the liquid phase (water and aqueous 0.2 M NaOH solution) at elevated pressure and the consequent increase in the concentration CO_2 in the solution phase is

Table 2 Rates of methanol and ethanol formation with radiation of different wavelengths (reproduced from Ref. [9], with permission from Elsevier; copyright 2009)

$BiVO_4$	Production rate[a] (μmol h^{-1})	300-W Xe arc lamp with UV cut-off filter	300-W Xe arc lamp without UV cut-off filter	36-W fluorescent lamp
Monoclinic	Ethanol	21.6	406.6	2.3
	Methanol	0	0	1.8
Tetragonal	Ethanol	1.1	4.9	0.6
	Methanol	0	0	0.6

[a] The rate was determined on the basis of average production rate after irradiation for 80 min

Journal : Small-ext 11164 | Dispatch : 26-10-2012 | Pages : 38
Article No. : 783 | LE | TYPESET
MS Code : | CP | DISK

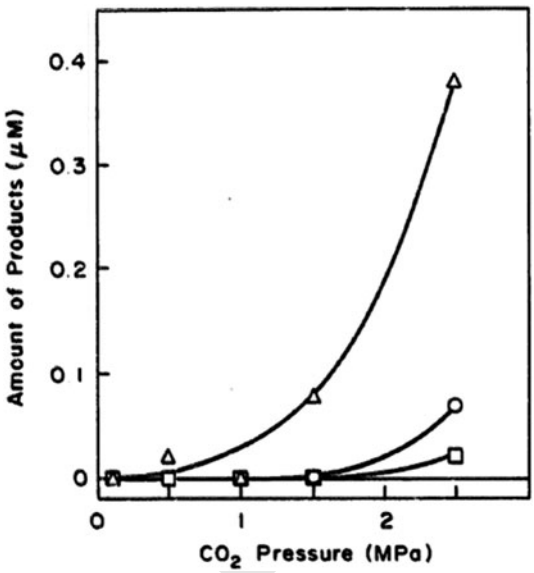

Fig. 5 Effect of CO_2 pressure on its photoreduction (medium, purified water; irradiation time, 24 h; catalyst, TiO_2): *open triangles* CH_4, *open circles* C_2H_4, *open squares* C_2H_6 (reproduced from Ref. [44], with permission from Elsevier; copyright 2009)

responsible for the observed increase in CO_2 reduction (Fig. 5). Similar effects of pressure have been observed by Hori et al. [46].

Effect of titania particle size, shape, and morphology

Kaneco et al. [47, 48] studied the photoreduction of CO_2 with TiO_2 powder in liquid CO_2 medium. Carbon dioxide has limited solubility in water. Also, reduction of CO_2 competes with hydrogen formation from water. To overcome this disadvantage liquid CO_2 has been investigated. The protonation reaction was performed by use of water after the end of illumination. The reduction product was exclusively formic acid. Tan et al. [49, 50] studied the photo catalytic reduction of carbon dioxide using TiO_2 pellets. Pellets increased contact area and adsorption capacity. The yield was significant compared with thin-film coating.

Koci et al. [51] studied the effect of TiO_2 particle size on photo catalytic reduction of carbon dioxide. As particle size was reduced, higher yields of methanol and methane over the TiO_2 nano particles were obtained on illumination with light. The optimum particle size corresponding to the highest yields of both products was 14 nm (Fig. 6). For particles with crystallite sizes smaller than 14 nm, conversion dropped, because of a combination of electronic (increase in recombination rates) and optical effects. The observed optimum particle size was a result of competing effects of specific surface area, charge-carrier dynamics, and light absorption efficiency.

Effect of type of photoreactor and reaction media

Koci et al. [52] studied the effect of reactor geometry on photoreduction of carbon dioxide using two annular batch reactors. The dependence of product yield on the reactor diameter and on the volume of the liquid phase confirmed that the

Journal : Small-ext 11164 | Dispatch : 26-10-2012 | Pages : 38
Article No. : 783 | LE | TYPESET
MS Code : | CP | DISK

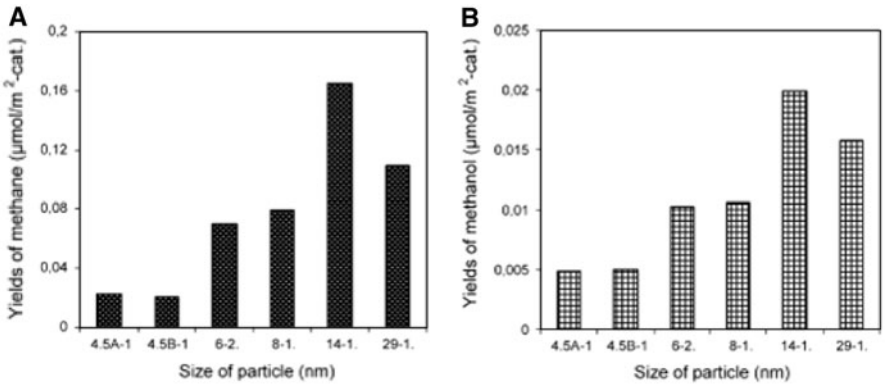

Fig. 6 Dependence of yields of methane (**a**) and methanol (**b**) on particle size of titania (after irradiation for 24 h) (reproduced from Ref. [49], with permission from Elsevier; copyright 2009)

requirement of perfect mixing is difficult with the annular configuration of the reactor. The highest yields from the photo catalytic reduction were achieved in a configuration in which the lamp just touches the surface of the liquid in the reactor and the configuration of the reactor was not annular.

Wu and coworkers [53] used an optical fibre reactor for photoreduction of CO_2 with H_2O using TiO_2, Cu/TiO_2, Ag/TiO_2, $Cu–Fe/TiO_2–SiO_2$, and dye-sensitized Cu–Fe/P25 coated on optical fibres. Compared with a traditional packed-bed reactor, an optical fibre provides a medium to transmit light uniformly throughout a reactor, which results in higher conversion (Table 3). In addition, a higher processing capacity is possible because the photocatalyst can be dispersed on the optical fibers with a large surface area in a given reactor volume.

When CO_2 present in the atmosphere dissolves in water it is mostly present in the form of carbonate. Many authors have studied photo catalytic reduction of carbonate with the formation of a variety of compounds. Ku et al. [54] studied the photo catalytic reduction of carbonate in aqueous solution by the UV/TiO_2 process. The photo catalytic reduction of carbonate proceeded faster in acidic solutions than in alkaline solutions. The main products of photo catalytic reduction of carbonate by the UV/TiO_2 reduction process were found to be methanol and methane.

Table 3 Product profile for photoreduction of CO_2 on TiO_2–CoPc systems (reproduced from Ref. [78], with permission from Elsevier; copyright 2009)

	Production rate[a] (μmol (g cat)$^{-1}$ h^{-1})	
	Ethylene	Methane
Cu (0.5 % *w/w*)–Fe (0.5 % *w/w*)TiO_2/glass plate	0.049	0.060
Cu (0.5 % *w/w*)–Fe (0.5 % *w/w*)/TiO_2/optical fiber	0.575	0.914
N3-dye-Cu (0.5 % *w/w*)–Fe (0.5 % *w/w*)/TiO_2/glass plate	0.033	0.148
N3-dye-Cu (0.5 % *w/w*)–Fe (0.5 % *w/w*)/TiO_2/optical fiber	0.562	0.847

[a] Production rates were determined on the basis of the average value after irradiation for 4 h. The artificial light was in the wavelength range 320–500 nm with intensity 225 mW cm^{-2}

Journal : Small-ext 11164 | Dispatch : 26-10-2012 | Pages : 38
Article No. : 783 | LE | TYPESET
MS Code : | CP | DISK

A Langmuir–Hinshelwood (L–H)-type kinetic equation was developed for modeling the photo catalytic reduction of carbonate.

Sayama et al. [55] investigated the effect of addition of carbonate salt on the photo catalytic decomposition of liquid water over Pt–TiO_2 catalyst. It was found that addition of carbonate salts to Pt-loaded suspensions led to highly efficient stoichiometric photo-catalytic decomposition of liquid water into H_2 and O_2. Neither pH nor cation contributes directly to water splitting. The presence of a high concentration of carbonate ions is essential for catalytic photo-decomposition of water. The carbonate ion affects both the Pt particles and the TiO_2 surface. The Pt was coated with titanium hydroxide compounds and, therefore, the rate of the back reaction (H_2O formation from H_2 and O_2) on the Pt was effectively suppressed in the presence of carbonate ions. On the other hand, the TiO_2 surface was readily coated with several types of carbonate species. It is believed that these carbonate species aid desorption of O_2 from the TiO_2 surface.

In place of pure water as the medium for dispersion of the catalysts, an aqueous solution of $KHCO_3$ [52] or NaOH has occasionally been used. Use of NaOH is beneficial because OH^- ions act as hole scavengers, thereby retarding electron–hole recombination and, simultaneously, the alkaline solution increases the solubility of CO_2 compared with pure water [56].

Photoreduction with other reductants

Some researchers have attempted to replace water with other reductants. This results in high reaction yield and high selectivity for the desired products by changing the mechanism. Liu et al. [57] conducted an experiment with CdS in different solvents, including water, methanol, ethanol, and 1-propanol, with dielectric constants of 80, 33, 24.3, and 20.1, respectively. The results indicated that if low-dielectric constant solvents or low-polarity solvents are used CO_2^- anion radicals can be strongly adsorbed on the surface via the carbon atom of another CO_2^- anion radical pre-sorbed on surface Cd sites because these radicals are not completely solvated by low-polarity solvents. Here, CO is produced as the major reduction product of CO_2. If a high-dielectric-constant solvent is used (e.g., water), the CO_2^- anion radicals can be greatly stabilized by the solvent, resulting in weak interactions with the photocatalyst surface. Similar effects of solvents have been observed on titania embedded in SiO_2 matrices [58]. Subsequently, the carbon atom of the radical tends to react with a proton to produce formic acid. Kaneco et al. [59] and later Dey et al. [60, 61] showed that photo-catalytic reduction of CO_2 using TiO_2 suspension in aqueous solutions containing 2-propanol as hole scavenger led predominantly to formation of methane.

photo catalytic reduction of CO_2 with water: state of the art

On semiconducting oxides

Inoue et al. [41] were the first to report the photo catalytic reduction of CO_2 in aqueous solutions to produce a mixture of formaldehyde, formic acid, methanol, and

Journal : Small-ext 11164 | Dispatch : 26-10-2012 | Pages : 38
Article No. : 783 | LE | TYPESET
MS Code : | CP | DISK

methane using a variety of wide-band-gap semiconductors, for example tungsten trioxide (WO_3), titanium dioxide (TiO_2), zinc oxide (ZnO), cadmium sulfide (CdS), gallium phosphide (GaP), and silicon carbide (SiC). These semiconductors were activated by both xenon and mercury lamp irradiation. Formaldehyde and methanol yields were the highest in the presence of SiC, behavior attributed to the position of the SiC CB relative to the $HCHO/H_2CO_3$ redox potential. The SiC CB edge lies at a higher position (more negative) than the $HCHO/H_2CO_3$ redox potential, which is believed to be responsible for the high rates of product formation. The absence of methanol when WO_3 was used as catalyst, with a CB at a position lower than the $HCHO/H_2CO_3$ redox potential, further indicates the effect of band-edge positions on CO_2 reduction (Fig. 4).

Investigations related to the photosynthesis reaction of CO_2 with water vapor to form CH_4 over metal-loaded $SrTiO_3$ have also been conducted. Because of its higher CB-edge position compared with the redox potential of CH_3OH/H_2CO_3, strontium titanate could effectively reduce carbon dioxide dissolved in an aqueous electrolyte [62, 63]. Halmann et al. [62] studied the doping of transition and noble metals such as Ru, V, and Cr on TiO_2 and observed that the rate of production of organic compounds such as formic acid, formaldehyde, and methanol increased when TiO_2 was doped with RuO_2.

Titania and titania loaded with metals or oxides as co-catalysts

Anpo et al. [64] studied the photo catalytic reduction of CO_2 with H_2O on a variety of titanium oxide catalysts. The anatase-type TiO_2 catalyst with large band gap and numerous surface-OH groups resulted in highly efficient formation of methane. The yields of the photo catalytic reactions were highly dependent on the kind of catalyst, the ratio of CO_2 to H_2O, and the reaction temperature. The best H_2O/CO_2 mole ratio for conversion of carbon dioxide was observed [64] to be 5 (Fig. 7).

Addition of Pt to the TiO_2 led to increased methane yield compared with methanol formation. Anpo et al. [64, 65] have studied in detail the use of highly dispersed titanium dioxide on glass for photo catalytic reduction of carbon dioxide. From direct detection of intermediate species by use of a variety of spectroscopic techniques, they proposed that methane formation resulted from the reaction between surface carbon radicals and atomic hydrogen (Scheme 6).

Use of Cu as a co-catalyst has been reported by Adachi and Mijuna [66]. Cu-loaded TiO_2 powder was suspended in a pressurized solution of CO_2 at ambient temperature; methane and ethylene were produced under Xe lamp illumination. Tseng et al. [56] also studied the effect of copper loading on titania. The methanol yield of 2.0 % (*w*/*w*) Cu/TiO_2 was 118 μmol/g after UV illumination for 6 h. The yield was much higher than those of sol–gel TiO_2 and Degussa P25. The redistribution of the electric charge and the Schottky barrier of Cu and TiO_2 facilitates electron trapping via supported Cu. The photo catalytic efficiency of Cu/TiO_2 was markedly increased because of reduction of the probability of re-combination of hole–electron pairs. The highest quantum and energy efficiency achieved were 10 and 2.5 %, respectively. Slamet et al. [67]. suggested that CuO may be the most active dopant compared with the other copper species. Because

Journal : Small-ext 11164 | Dispatch : 26-10-2012 | Pages : 38
Article No. : 783 | LE | TYPESET
MS Code : | CP | DISK

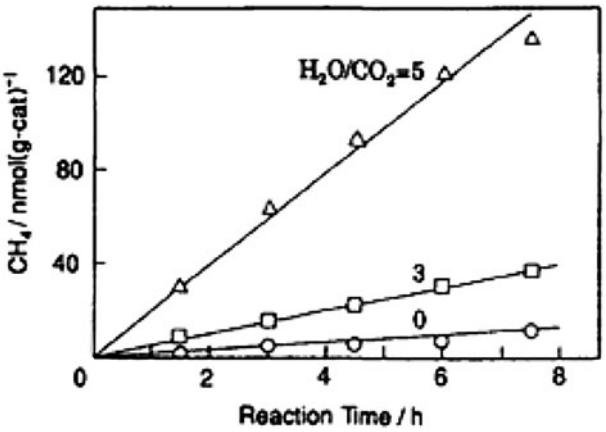

Fig. 7 Time profiles of the photo catalytic reaction of CO_2 (0.05 mmol g^{-1}) and H_2O to produce CH_4 on titanium dioxide anchored on PVG, and the effect of H_2O to CO_2 ratio on the yields of the products. *Numbers* represent the ratio of H_2O to CO_2 (reproduced from Ref. [61], with permission from Elsevier; copyright 1995)

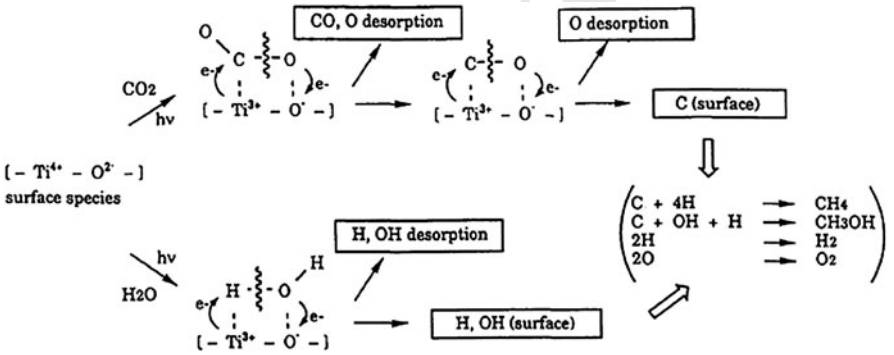

Scheme 6 Schematic representation of the photo catalytic reduction of CO_2 with H_2O on anchored titanium dioxide (reproduced from Ref. [61], with permission from Elsevier; copyright 1995)

Cu_2O has the highest positive redox potential value of Cu^+, Cu_2O dopant should effectively act as an electron trapper to prohibit electron–hole recombination. However, owing to the relatively strong interaction between TiO_2 and the dopant particle implanted in the vacant sites of TiO_2, the dopant with more positive redox potential efficiently catches electrons from the CB edge. Consequently the dopant-trapped electrons are more difficult to transform to the adsorbed species on catalyst surface which may, therefore, be a center for electron–hole recombination.

Titania per se is active in photo catalytic reduction of CO_2 with H_2O, but the rates are extremely low because its CB edge is not suitable for water and CO_2 reduction, though it can readily oxidize water [68]. Promotion with co-catalysts, for example Pt [69] (Fig. 8), Ru [70], Rh [71], Ni [43] and Ag [72] (Fig. 9) vastly enhances the rate in several ways, for example by charge separation, retarding re-combination,

Journal : Small-ext 11164 | Dispatch : 26-10-2012 | Pages : 38
Article No. : 783 | LE | TYPESET
MS Code : | CP | DISK

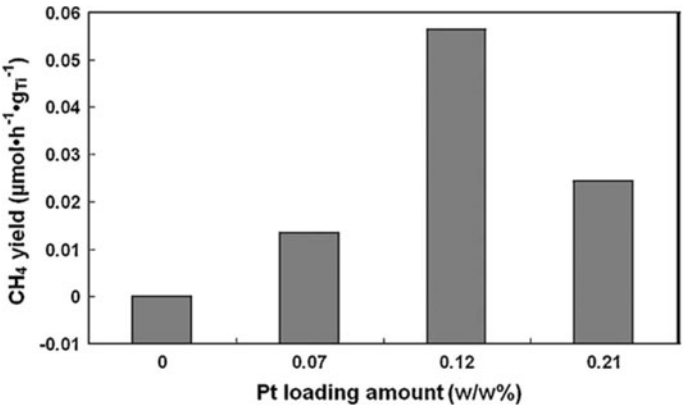

Fig. 8 Effect of Pt metal content in Pt/TO-NP on methane yield in photo catalytic reduction of CO_2 after irradiation for 7 h at 323 K $H_2O/CO_2 = 0.02$ (reproduced from Ref. [66], with permission from Elsevier; copyright 2009)

and trapping of charge carriers, besides activation of CO_2 and water reduction and facilitating further surface transformations leading to hydrocarbon products.

Effects of bi-metallics on TiO_2 were also studied by Luo et al. [73] for CO_2 reduction on copper and cerium-co-doped titanium dioxide. photo catalytic copper and cerium co-doped titanium dioxide were prepared via the equivalent-volume incipient wetness impregnation method. Methanol yield could rapidly reach 180.3 μmol/g catalyst. Ce atoms activated H_2O and CO_2 molecules whereas Cu atoms act as the channel for photoelectrons in real time and prevent recombination of electrons and holes.

A significant breakthrough in the photo catalytic reduction of gas phase CO_2 by solar radiation has recently been achieved by Varghese et al. [68], by use of nitrogen-doped TiO_2 nano tube arrays and co-catalysis with copper and/or Pt nano particles—CO_2 and water vapor were reduced to methane and other hydrocarbons under natural sunlight. The yield of methane was reported to be 111 ppm cm^{-2} h^{-1} (160 μl/g h) with quantum efficiency of 0.74 % (Fig. 10). The high rate of CO_2 conversion is because the high surface area and nano scale wall thickness of the nano tubes enables the surface species to readily receive both charge carriers generated near the surface, because of wave function overlap, and those generated deep inside the wall, via diffusion.

Titanates with layered structure

Guan et al. [74] studied the reduction of CO_2 with water over a hybrid catalyst comprising a Pt-loaded $K_2Ti_6O_{13}$ photocatalyst combined with a Fe-based catalyst supported on a de-aluminated Y-type zeolite (Fe–Cu–K/DAY). In this reaction system, the Pt/$K_2Ti_6O_{13}$ catalyst decomposes water to produce H_2 and the Fe–Cu–K/DAY catalyst reduces CO_2 with the resulting H_2 into organic compounds. When the reaction temperature is increased from room temperature to 600 K by

Journal : Small-ext 11164 | Dispatch : 26-10-2012 | Pages : 38
Article No. : 783 | LE | TYPESET
MS Code : | CP | DISK

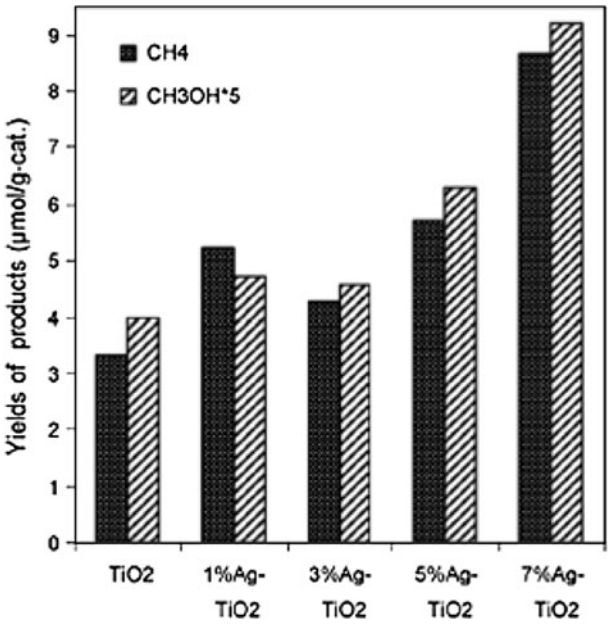

Fig. 9 Dependence of product yields on Ag content of Ag/TiO_2 (after 24 h) (reproduced from Ref. [69], with permission from Elsevier; copyright 2010)

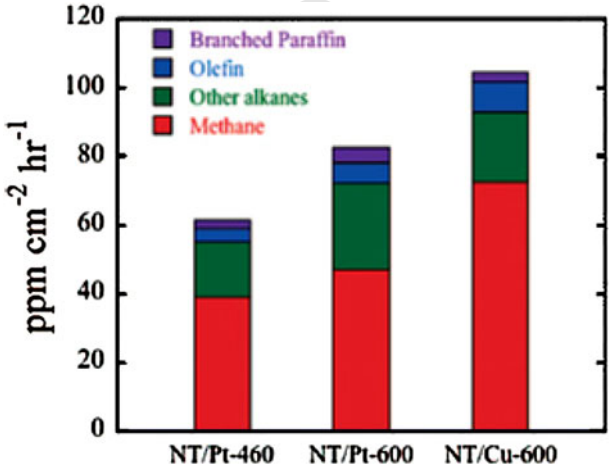

Fig. 10 Rate of hydrocarbon generation by N-doped TiO_2 nano tube arrays with Pt (NT/Pt) and Cu (NT/Pt) co-catalysts, annealed at 460 or 600 °C, as indicated (reproduced from Ref. [65], with permission from the American Chemical Society; copyright 2009)

560 concentrating the solar irradiation, the product yield of hydrogen increased from
561 13.7 to 20.5 μmol/g h. Formic acid, methanol, and ethanol were also obtained.
562 Guan et al. [75] also reported use of a Pt-loaded $K_2Ti_6O_{13}$ photocatalyst combined

Journal : Small-ext 11164 | Dispatch : 26-10-2012 | Pages : 38
Article No. : 783 | LE | TYPESET
MS Code : | CP | DISK

with a CO_2 hydrogenation catalyst, Cu/ZnO. When the composite catalyst was used under concentrated sunlight, CH_3OH was successfully formed in addition to the above products. Guan et al. [76] also investigated reduction of CO_2 over zero-valent Fe^0 and Fe^0-based composites in an aqueous solution at room temperature. It was found that H_2, with a small amount of hydrocarbons, can be effectively evolved from water over zero-valent Fe^0 in the presence of gaseous CO_2. When the Fe^0 was combined with Cu, K, and Al, hydrocarbons such as CH_4 and C_3H_8 and alcohols such as CH_3OH and C_2H_5OH were also produced. XPS, XRD, and photo-emission yield measurements revealed that the Fe^0 surface and the bulk was oxidized to Fe_3O_4 and other possible oxides during the reaction. This corrosion process is promoted by the dissolution of CO_2 in water and the resulting protons oxidize Fe^0 to evolve H_2. Moreover, the evolved H_2 serves as the reactant for hydrogenation of CO_2 on the active site of Fe^0, especially for the Fe^0–K–Al and Fe^0–Cu–K–Al composites.

Titania dispersed on different meso/nano porous and macrocyclic matrices

Ulagappan et al. [77, 78] used Ti-silicalite molecular sieves as a catalyst for 266 nm UV laser radiation-induced reduction of CO_2 and H_2O gas mixtures, obtaining HCOOH, CO and $HCOOCH_3$. The origin of the products was studied by IR spectroscopy, which indicated that CO originated from secondary photolysis of HCOOH whereas $HCOOCH_3$ was the result of spontaneous Tishchenko reaction of CH_2=O.

Photocatalysts prepared within the zeolite cavity and framework have a unique local structure and high selectivity in photoreduction. Titanium oxide species embedded within a zeolite framework have been found to exist as isolated tetrahedral titanium oxide species. These Ti-containing zeolite catalysts had high photo catalytic efficiency and selectivity for formation of methanol. Anpo et al. [79] conducted CO_2 photoreduction using TiO_2 in well-dispersed isolated state in Y-zeolite cavities, in tetrahedral co-ordination, and observed high selectivity for methanol formation, whereas aggregates of titania in the octahedral state on zeolites and bulk TiO_2 resulted in methane formation. Surface structure/surface co-ordination of titania (determined by EXAFS) has a profound effect on the selectivity CO_2 photoreduction to methanol, as shown in Fig. 11. Ti-MCM-48 mesoporous zeolite, with large pores and three dimensional channels, was more active and selective in methanol formation than Ti-MCM-41 (Fig. 12), with a one-dimensional pore structure [80, 81].

Macrocyclic ligands, for example Pcs and Prs, have high absorption coefficients in the solar spectrum, especially in the visible region, and good chemical stability; they are, hence, preferred for sensitization of titania and other semiconductors [7–12]. Liu et al. [12, 82] reported photo catalytic reduction of carbon dioxide using sol–gel-derived titania-supported CoPc catalysts. In-situ synthesis results in the formation of isolated CoPc species (within the confined space of mesoporous titania) which effectively absorb visible light enabling ultrafast injection of electrons from the excited state into the CB of the titania support, thus helping charge-carrier separation and increasing photo-conversion efficiency [12, 82].

Journal : Small-ext 11164 | Dispatch : 26-10-2012 | Pages : 38
Article No. : 783 | LE | TYPESET
MS Code : | CP | DISK

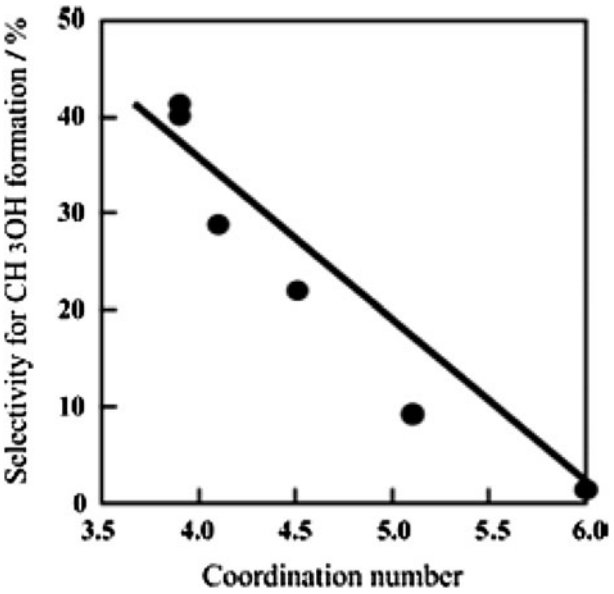

Fig. 11 Relationship between the selectivity of methanol formation in the reduction of CO_2 with H_2O and the co-ordination number of TiO_2 species determined by EXAFS investigation (reproduced from Ref. [61], with permission from Elsevier; copyright 2003)

Because the reported band gap for TiO_2 is 3.22 vs. 2.14 eV for CoPc, such a sensitization process is highly feasible. CO_2 photoreduction data presented in Table 4 show that the in-situ CoPc/TiO_2 catalyst is more active than a simple mechanical mixture of CoPc and TiO_2, indicating a co-operative effect between dispersed CoPc and the titania surface enables effective transfer of photogenerated electrons.

Xia et al. [83] studied the reduction of CO_2 with H_2O using multi-walled carbon nano tube [MWCNT]-supported TiO_2. The catalysts were prepared by both the sol–gel and hydrothermal methods. In the sol–gel method, the MWCNTs were coated with anatase TiO_2 nano particles; in the hydrothermal method, rutile TiO_2 nano rods were uniformly deposited on the MWCNTs. The composite catalysts prepared by the sol–gel method resulted mainly in the formation of C_2H_5OH whereas HCOOH

Table 4 Rate of production of methane and ethylene over TiO_2-based catalysts under artificial light—effect of the type of photoreactor on reaction rate (reproduced from Ref. [51], with permission from Elsevier; copyright 2008)

Catalyst	Product yield (μmol/g catalyst)			
	HCOOH	CH_3OH	HCHO	Total organic carbon
TiO_2	221	–	–	221
1 % (*w*/*w*) CoPc/TiO_2	450.6	12.1	38.5	501.2
0.7 % in-situ CoPc/TiO_2	1487	93	134.3	1714

Journal : Small-ext 11164 | Dispatch : 26-10-2012 | Pages : 38
Article No. : 783 | LE | TYPESET
MS Code : | CP | DISK

was the major product on the sample prepared by the hydrothermal method. It is likely that the preparation methods adopted may expose surface titania in different co-ordination and/or environments, facilitating surface transformations via different pathways, leading to changes in product distribution and/or selectivity [84].

CO_2 photoreduction using external hydrogen

Many researchers have studied the photo catalytic reduction of CO_2 using external hydrogen. Lo et al. [85] studied the photoreduction of carbon dioxide with H_2 and H_2O over TiO_2 and ZrO_2 in a circulated photo catalytic reactor. Experimental results indicated that the highest yield in the photoreduction of CO_2 was obtained using TiO_2 with $H_2 + H_2O$ and ZrO_2 with H_2. Photoreduction of CO_2 over TiO_2 with $H_2 + H_2O$ formed CH_4, CO, and C_2H_6 with yields of 8.21, 0.28, and 0.20 μmol/g, respectively, whereas photoreduction of CO_2 over ZrO_2 with H_2 formed CO with a yield of 1.24 μmol/g. The detected reaction products supported the proposition of two reaction pathways for photoreduction of CO_2 over TiO_2 and ZrO_2 with H_2 and H_2O, respectively. A one-site L–H kinetic model was used to simulate the rate of photoreduction of CO_2.

Mixed metal oxide catalysts for CO_2 photoreduction

Tsuneoka et al. [86] performed CO_2 photoreduction over MgO, CaO, ZrO_2, Ga_2O_3, and Al_2O_3. Ga_2O_3 had the highest photo catalytic activity in this process, and CO gas was selectively generated at room temperature and atmospheric pressure. The amount of CO gas evolved depended not only on the amount of CO_2 adsorbed but also on the amount of H_2 adsorbed on Ga_2O_3 (Scheme 7). The chemisorbed CO_2

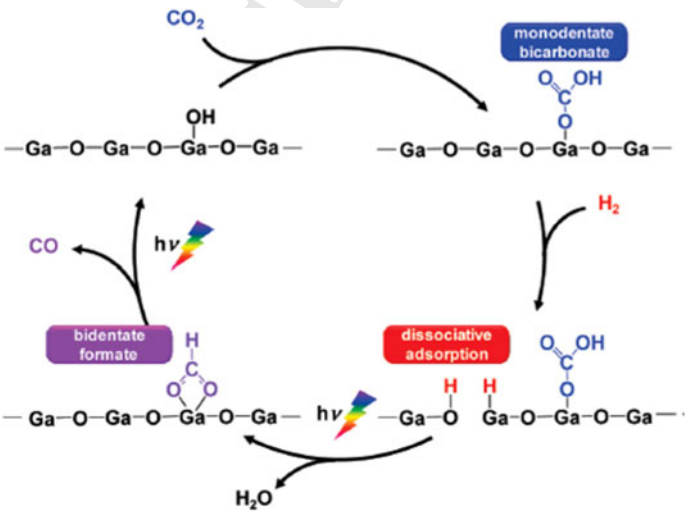

Scheme 7 Mechanism of photo catalytic reduction of CO_2 over Ga_2O_3 in the presence of hydrogen (reproduced from Ref. [82], with permission from the American Chemical Society; copyright 2010)

Journal : Small-ext 11164 | Dispatch : 26-10-2012 | Pages : 38
Article No. : 783 | LE | TYPESET
MS Code : | CP | DISK

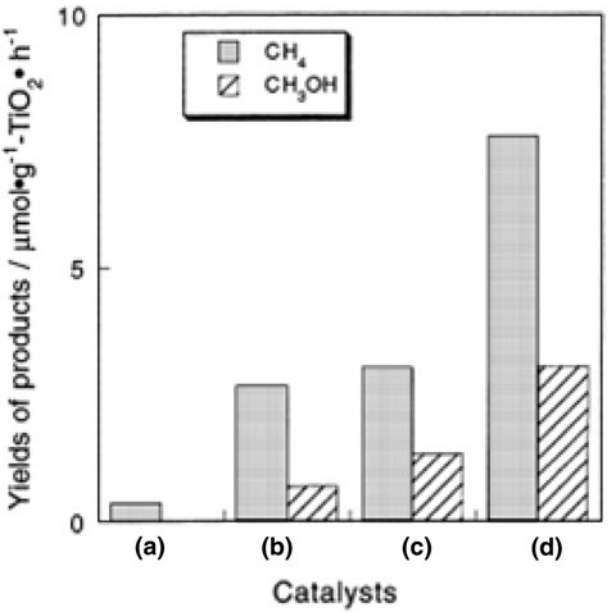

Fig. 12 Yields of CH_4 and CH_3OH in the photo catalytic reduction of CO_2 with H_2O on TiO_2 powder (*a*), and on TS-1 (*b*), Ti-MCM-41 (*c*), and Ti-MCM-48 (*d*) zeolite catalysts (reproduced from Ref. [77], with permission from Elsevier; copyright 1998)

species involved in the photo catalytic reduction of CO_2 over Ga_2O_3 was not the bi-dentate bicarbonate species but the mono-dentate bicarbonate species. Dissociatively adsorbed hydrogen on Ga_2O_3 reduced the mono-dentate bicarbonate to the bi-dentate formate under photoirradiation (Fig. 13). The bi-dentate formate, which was an intermediate in the photo catalytic reduction, decomposed to CO. An L–H-type mechanism is proposed for photo catalytic reduction of CO_2 over Ga_2O_3, which is not the case for ZrO_2 or MgO.

Teramura et al. [87] performed photo catalytic reduction of CO_2 using H_2 as reductant over $ATaO_3$ photocatalysts (A = Li, Na, K). Only CO gas was generated over all samples under photoirradiation. The photo catalytic activity was higher in the order $LiTaO_3 > NaTaO_3 > KTaO_3$ (Fig. 14). This order of the photo catalytic activity was consistent with that of the E_g (band gap) values. For $ATaO_3$ the amount

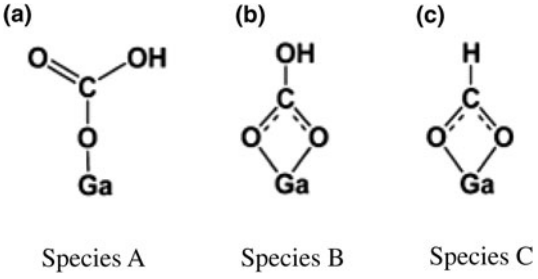

Fig. 13 Adsorbed CO_2 species on Ga_2O_3: (**a**) mono-dentate bicarbonate, (**b**) bi-dentate bicarbonate, (**c**) bi-dentate formate (reproduced from Ref. [82], with permission from the American Chemical Society; copyright 2010)

Journal : Small-ext 11164 | Dispatch : 26-10-2012 | Pages : 38
Article No. : 783 | LE | TYPESET
MS Code : | CP | DISK

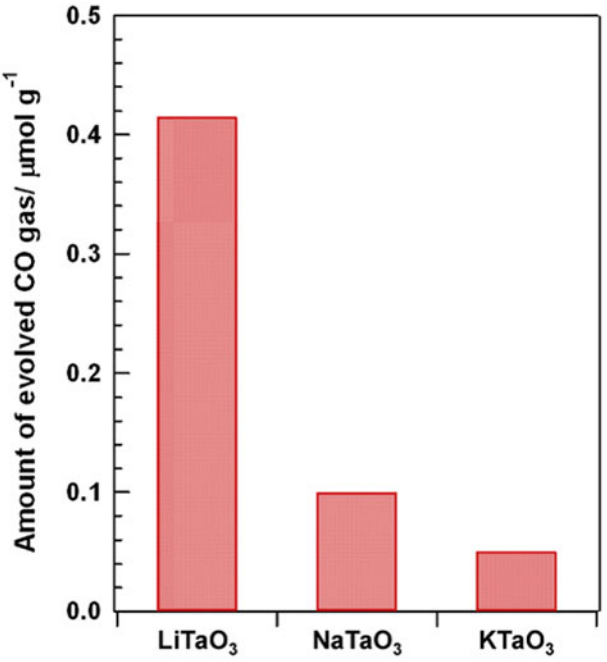

Fig. 14 Amount of CO gas evolved in photo catalytic reduction of CO_2 with external H_2 as reductant over $ATaO_3$ (A = Li, Na, K) after photoirradiation for 24 h (reproduced from Ref. [83], with permission from Elsevier; copyright 2010)

of CO gas evolved is highly dependent on the amount of chemisorbed CO_2. In addition, photo catalytic activity increased with increasing the temperature of calcination of $LiTaO_3$. This means that smooth charge separation in the $LiTaO_3$ photocatalyst and chemisorption of CO_2 on the surface contribute to effective reduction of CO_2 in the presence of H_2.

Catalyst systems other than TiO_2

Watanabe [88] studied the photosynthesis of methanol and methane from CO_2 and H_2O molecules on a ZnO surface. Photochemical synthesis of methanol and methane from CO_2 and H_2O was observed at 5 °C by irradiating ZnO powder with visible light under high pressure (25–35 kg/cm^2) CO_2 gas. Using a 75 W Xe lamp the best conversion efficiency was approximately 6 % relative to reactant H_2O molecules.

Kanemoto et al. [89] studied the photoreduction of carbon dioxide over ZnS quantum crystallites. Dissolution of CO_2 in water gives an aqueous solution of pH 3.7 under a pressure of 1 atm. ZnS is unstable under acidic conditions, decomposing into H_2S and Zn^{2+} on reaction with the acid. Freshly prepared colloidal ZnS suspensions effectively catalyze photoreduction of CO_2 in water at pH 7 with NaH_2PO_2 in the presence of Na_2S under UV irradiation. Wang et al. [90]

Journal : Small-ext 11164 | Dispatch : 26-10-2012 | Pages : 38
Article No. : 783 | LE | TYPESET
MS Code : | CP | DISK

achieved photo catalytic evolution of H_2 from water in the presence of carbon dioxide over $NiO/Ca_2Fe_2O_5$. It is believed that CO_2 may react with water to form HCO_3^- and CO_3^{2-}, which promote the scavenging of holes by OH, and thus enhance the photo catalytic activity. At the same time, some of the CO_2 is photo catalytically reduced to formic acid.

Ahmed et al. [91] studied the photo catalytic conversion of carbon dioxide into methanol by use of zinc–copper–M(III) (M = Al, Ga) layered double hydroxides (LDHs). These LDH compounds were used as photocatalysts to convert gaseous CO_2 (2.3 kPa) to methanol or CO under UV–visible light by use of hydrogen. Zn–Al LDH was the most active for CO_2 photoreduction and the major product was CO, formed at a rate of 620 nmol h^{-1} g^{-1} cat, whereas methanol was the major product formed by inclusion of Cu in the LDH photocatalysts; for example, it was formed at a rate of 170 nmol h^{-1} g^{-1} catalyst by use of Zn–Cu–Ga photocatalyst.

Yan et al. [92] studied the CO_2 photoreduction using mesoporous $ZnGa_2O_4$. A reactive templating route for preparation of mesoporous $ZnGa_2O_4$ at room temperature has been reported. If RuO_2 is used as co-catalyst the as-prepared mesoporous $ZnGa_2O_4$ has high photo catalytic activity in the conversion of CO_2 into CH_4 under light irradiation, because of strong gas adsorption and the large specific surface area of the mesoporous photocatalyst.

Kinetics and mechanism of CO_2 photoreduction with water

Formation of different transient surface species and their transformation on TiO_2 during photo catalytic reduction of CO_2 by water was traced by Anpo et al. [64] by use of ESR, EXAFS, and other spectroscopic techniques. Ti^{3+}, H, C, and CH_3 radicals were detected by ESR studies performed at 77 K. The charge-transfer excited state $(Ti^{3+}–O^-)^3*$ with Ti in tetrahedral co-ordination, formed by absorption of light energy, was proposed as the active site on which CO_2 is reduced to CO and C, and which, on addition of active surface hydrogen, forms hydrocarbons. Further mechanistic pathways have also been elucidated (Scheme 6).

These observations find support in a recent publication by Dimitrijevic et al. [93], who reported detailed low-temperature ESR measurements on TiO_2 nano particles dispersed in aqueous alkaline solutions which indicated formation of H atoms and *OH radicals, in addition to methyl ($^{\bullet}CH_3$) and methoxy ($^{\bullet}CH_3O$) radicals, on the surface. Formation of surface formate species is proposed as the initial step, in accordance with Scheme 8, below.

$$CO_2 + 2e^- + H^+ \rightarrow HCOO^- \quad (22)$$

On the basis of in-situ IR spectroscopic studies Wu and Huang [94, 95] proposed a different route involving HCOOH as the primary intermediate. IR absorption bands arising from bicarbonate, carbonate, formate, formaldehyde, and methoxy species on the TiO_2 surface have been observed, indicating transformation pathways in the same order (Scheme 9).

Journal : Small-ext 11164 | Dispatch : 26-10-2012 | Pages : 38
Article No. : 783 | LE | TYPESET
MS Code : | CP | DISK

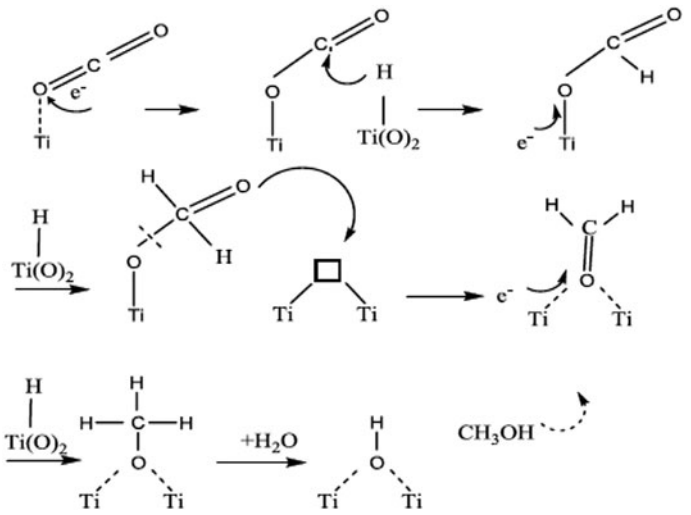

Scheme 8 Proposed mechanism of photo catalytic CO_2 reduction over TiO_2 (reproduced from Ref. [90], with permission from Springer Science and Business Media; copyright 2009)

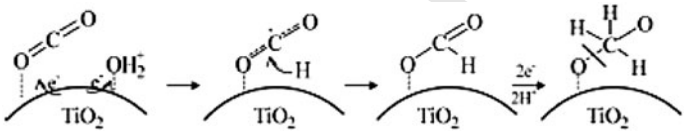

Scheme 9 Proposed mechanism of photo catalytic transformation of CO_2 to methoxy radical over TiO_2 in the presence of dissociated and/or bound water (reproduced from Ref. [89], with permission from the American Chemical Society; copyright 2011)

Accordingly, methanol is formed via surface methoxy species. Earlier, Subrahmanyam et al. [96] (for mixed oxides of titania) and Sasirekha et al. [70] (for Ru supported on TiO_2 dispersed on SiO_2) proposed similar surface reaction pathways.

Although mechanisms proposed to explain the formation of C_1 organic compounds are reasonably well accepted, the pathways leading to formation of C_2 and $>C_2$ compounds are not clearly understood. Dimerization of surface C_1 species has been proposed as a possible route for formation of C_2 hydrocarbon products [97], although direct experimental evidence of this is lacking.

Ulagappan and Frei [77, 78] performed a mechanistic study of the reaction with methanol as electron donor on Ti-silicalite using in-situ FT-IR spectroscopy and traced the reaction pathway using isotopic labeling studies with $C^{18}O_2$, $^{13}CO_2$, and $^{13}CH_3OH$. HCOOH was identified as the primary product, pyrolysis of which gives CO. In the absence of methanol, water was confirmed as the electron donor.

A recent publication by Yang et al. [98, 99] on photo catalytic reduction of CO_2 using Ti-SBA-15 reports investigation of the effects on product patterns of varying feed composition, with a view to understanding the reaction mechanism. In particular, addition of CO, H_2, in the place of H_2O, methanol, and formaldehyde

Journal : Small-ext 11164 | Dispatch : 26-10-2012 | Pages : 38
Article No. : 783 | LE | TYPESET
MS Code : | CP | DISK

was studied in detail. Whereas CH_4, C_2H_4, and C_2H_6 were produced at reasonable rates by use of CO + H_2O, with a mixture of CO + H_2, the rates of reaction were very low. It was concluded that H_2O was a more efficient reductant with CO_2 or CO than H_2. CH_3OH was not a significant product, and when added with the feed it did not increase the reaction rate. Similarly, added formic acid also did not enhance product formation. These observations rule out methanol or formic acid as intermediates in the formation of hydrocarbons on Ti-SBA-15. However, added formaldehyde underwent facile conversion to hydrocarbon products. On the basis of detailed analysis of the products, it was proposed that CO_2 photoreduction proceeds through formation of CO in the initial stages, followed by its conversion to formaldehyde, which in turn is converted to other hydrocarbon products. The Ti–OH site, which on photo-activation is converted to [Ti(III)–O]*, is regarded as the active site [77]. A reaction mechanism (Scheme 10) which does not involve formic acid as intermediate has been proposed.

Yang et al. [98, 99] observed that the backward reaction, i.e., oxidation of hydrocarbons back to CO_2 and water, proceeds to a significant extent. This implies that the oxygen produced by the splitting of water, which is responsible for the backward reaction, must be removed effectively to increase hydrocarbon yields. Means of separating physically the oxidation and reduction sites would be crucial in this respect. It is clear that the reaction mechanism is quite complex and depends on the type of the catalysts and/or active sites.

An in-depth understanding of the reaction mechanism and the rapid deactivation of the photocatalyst would be helpful in the development of superior catalysts for this process, which has the potential to emerge as a sustainable route for production of fuels and chemicals.

Kinetic models for photo catalytic reduction of CO_2 with water on titania have been reported by Lo et al. [85] and Tan et al. [100]. Both authors have used a single site L–H-type kinetic model to simulate the process. Lo et al. [85] successfully validated their model with a pseudo-first-order reaction rate equation by use of experimental data. Tan et al. [100] adopted the reaction scheme involving formation of surface carbon radicals, as proposed by Anpo et al. [64], and could predict rates

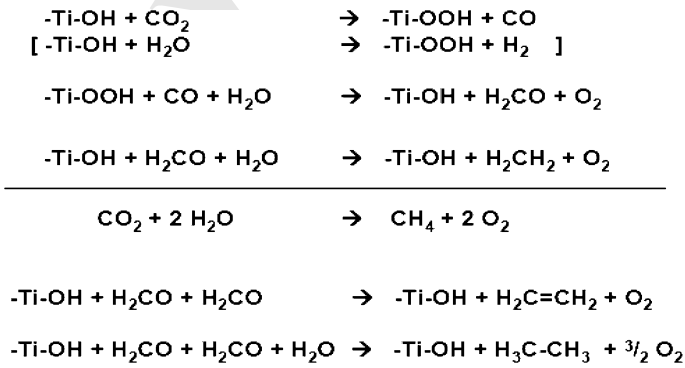

Scheme 10 Mechanism for photo catalytic reduction of CO_2 with water on Ti-SBA-15 (reproduced from Ref. [94], with permission from Elsevier; copyright 2011)

Journal : Small-ext 11164 | Dispatch : 26-10-2012 | Pages : 38
Article No. : 783 | LE | TYPESET
MS Code : | CP | DISK

of formation of methane and hydrogen. Koci et al. [101], by applying the L–H model, checked the suitability of the two reaction mechanisms proposed, i.e., one by Anpo et al. [64] and the other by Wu and Huang [94] and observed that their model supports Anpo's mechanism wherein CO is proposed as the primary intermediate.

Deactivation of catalysts

In some cases [69, 70, 102, 103] the catalysts reported for photoreduction of CO_2 tend to become deactivated within short a period, although in a few cases activity beyond 20 h has been reported. Transformation of photo-activated CO_2 to hydrocarbons proceeds through several hydrocarbon intermediates, whose identity or nature is yet to be established. Accumulation of these intermediates on the catalyst surface and blocking of the active sites is a major reason for catalyst deactivation. For catalyst nano particles dispersed in liquid media, coagulation and reduction in light absorption power [70] and changes in the oxidation state of metal ions [102] may lead to catalyst deactivation. Regeneration with air helps to restore the activity. However the phenomenon of catalyst deactivation in this process needs further study, especially when large-scale applications of this process are desired.

CO_2 photoreduction in the homogeneous phase by use of metal complexes

Use of transition metal complexes as catalysts for CO_2 photoreduction [104] has several advantages, for example facile synthetic routes, well-defined structure which can be easily adapted to suit the application, metal centers amenable to redox processes, ability to activate CO_2, and, above all, can be photo-active themselves, although an external sensitizer could be used if necessary. Homogeneous catalyst systems useful for this process can be divided into several groups:

1. $Ru(bpy)_3^{2+}$-based catalysts that can act both as photosensitizer and catalyst
2. $Ru(bpy)_3^{2+}$-based catalysts as photosensitizer and another metal complex as catalyst
3. $Ru(bpy)_3^{2+}$ and $Ru(bpy)_3^{2+}$-type complexes as photo sensitizers in micro-heterogeneous systems
4. $ReX(CO)_3(bpy)$ or a similar complex both as photosensitizer and catalyst;
5. Prs both as photosensitizer and catalyst; and
6. Organic photosensitizers and a metal complex as catalysts.

An advantage of these types of catalyst is that they are amenable to comprehensive spectroscopic characterization at various stages of the process, which could help in tracing reaction pathways and devising means of improving process efficiency. Bipyridyl complexes of Ru and Re (complexes of the type $Ru(bpy)_2(CO)X^{n-}$ (where bpy is 2,2-bipyridine, X = CO, Cl, H, etc.) and Co macrocycles $(CoHMD)^{2+}$ (where HMD is 5,7,7,12,14,14-hexamethyl-1,4,8,11-

Journal : Small-ext 11164 | Dispatch : 26-10-2012 | Pages : 38
Article No. : 783 | LE | TYPESET
MS Code : | CP | DISK

Table 5 Metal complexes as catalysts for photoreduction of CO_2 (reproduced from Ref. [104], with permission from Elsevier; copyright 1999)

Sensitizer	Catalyst or relay	Donor	Product(s)	Φ[a] mol Einstein^{-1}
$Ru(bpy)_3^{2+}$		TEOA	$HCOO^-$	0.049[b]
$Ru(bpy)_3^{2+}$		TEOA	$HCOO^-$	0.096[c]
$Ru(bpy)_3^{2+}$	MV^{2+}	TEOA	$HCOO^-$	0.01
$Ru(bpy)_3^{2+}$	Co^{2+}/bpy	TEA	CO, H_2	
$Ru(bpy)_3^{2+}$	Co^{2+}/Me_2phen	TEA	CO, H_2	0.012 (CO) 0.065 (H_2)
$Ru(bpy)_3^{2+}$	$Ru(bpy)_2(CO)_2^{2+}$	TEOA	$HCOO^-$	0.14
$Ru(bpy)_3^{2+}$	$Ru(bpy)_2(CO)_2^{2+}$	BNAH	$HCOO^-$, CO	0.03 ($HCOO^-$) 0.15 (CO)
$Ru(bpy)_3^{2+}$	$Ru(bpy)_2(CO)(H)^+$	TEOA	$HCOO^-$	0.15
$Ru(bpy)_3^{2+}$	$Ru(bpy)_2(CO)(X)^{n+}$, X = Cl and CO	TEOA	$HCOO^-$	
$Ru(bpy)_3^{2+}$	$CoHMD^{2+}$	H_2A	CO, H_2	
$Ru(bpy)_3^{2+}$	$Nicyclam^{2+}$	H_2A	CO, H_2	0.001 (CO)
$Ru(bpy)_3^{2+}$	$NiPr\text{-}cyclam^{2+}$	H_2A	CO, H_2	Ca. 0.005 (CO)
$Ru(bpy)_3^{2+}$	Ru colloid	TEOA	CH_4	10^{-4} (CH_4)[d]
$Ru(bpy)_3^{2+}$	$Bipyridinium^+$, Ru or Os colloid	TEOA	CH_4, H_2	10^{-4} (CH_4)[d] 10^{-3} (H_2)[d]
$ReCl(bpy)(CO)_3$		TEOA	CO	0.14
$ReBr(bpy)(CO)_3$		TEOA	CO	0.15
$[ReP(OEt)_3(bpy)(CO)_3]^+$		TEOA	CO	0.38
p-Terphenyl	$Cocyclam^{3+}$	TEOA	CO, $HCOO^-$, H_2	0.25[d] (CO + $HCOO^-$)
p-Terphenyl	$CoHMD^{2+}$	TEOA	CO, $HCOO^-$, H_2	
Phenazine	$Cocyclam^{3+}$	TEOA	$HCOO^-$	0.07[d]
FeTPP		TEA	CO	
CoTPP		TEA	$HCOO^-$, CO	

TEOA, triethanolamine; MV^{2+}, methylviologen; TEA, triethylamine; bpy, 2,2′-bipyridine; Me_2phen, 2,9-dimethyl-1,10-phenanthroline; BNAH, 1-benzyl-1,4-dihydronicotinamide; H_2A, ascorbic acid; cyclam, 1,4,8,11-tetraazacyclotetradecane; Pr-cyclam, 6-((NR)pyridin-4-yl)methyl-1,4,8,11-tetraazacyclotetradecane, where R is *p*-methoxybenzyl or benzyl; TPP, 5,10,15,20-tetraphenyl-21*H*,23*H*-porphine

[a] Unless otherwise noted, the quantum yield of product formation is defined as the rate of formation divided by the light intensity

[b] With 15 % water in DMF

[c] With 15 % water and excess bpy in DMF

[d] Assuming two (or eight) photons produce one molecule of the product

799 tetraazacyclotetradeca-4,11-diene) have been investigated extensively for CO_2
800 photoreduction. Typical examples of Ru, Re Co, and Fe complexes and macrocycles
801 studied for photoreduction are given in Table 5.

Journal : Small-ext 11164 | Dispatch : 26-10-2012 | Pages : 38
Article No. : 783 | LE | TYPESET
MS Code : | CP | DISK

Most of the catalysts facilitate reduction of CO_2 to CO and/or formate only and some generate hydrogen, although formation of C_1 and C_2 compounds has been observed in the presence of metallic colloids. Willner et al. [105] observed that Ru and Os colloids, in homogeneous phase, with $Ru(bpy)_3^{2+}$ as photo-sensitizer, triethanolamine, as electron donor, and *N*,*N*′-dimethyl 2,2-bipyridinium as charge relay, led to the conversion of CO_2 to methane, ethylene, and hydrogen. However, changing over to Ru(II)tris(bipyrazine) as sensitizer results in methane, ethylene, and ethane but with no evolution of hydrogen. H_2 evolution is thus inhibited by addition of bipyrazine, whereas methane formation is inhibited by addition of thiols. Tuning product selectivity is possible with proper selection of photo-sensitizer, charge relay, and metallic colloids. There are, however, several inherent limitations, for example poor stability of the metal complexes during reaction, deactivation of the catalyst, low conversion, and low reaction rates (typically, TON <300 and TOF <20 h^{-1}), reaction pathways yet to be established, absorption of light in a limited region of the solar spectrum, need to shift from noble metal-based (Ru, Re) to transition metal based (Fe, Co, and Ni) catalysts, avoiding the use of sacrificial donors, and coupling with water oxidation catalysts [106]. A recent perspective on these issues by Grills and Fujita [107] reveals some developments, for example conducting reactions with supramolecular catalyst systems in supercritical CO_2 ($scCO_2$) or in $scCO_2$–ionic liquid mixtures.

Recent trends

Developing alternative catalysts, improving hydrocarbon yields, and arresting catalyst deactivation are the focal points for current research efforts in this area. A notable development is the application of nano-sized titania dispersed on a mesoporous silica matrix of large surface area and pore volume as catalyst for photo catalytic reduction of CO_2 with H_2O [70, 102, 103]. A mesoporous structure is expected to facilitate faster electron transfer within the matrix and retard charge recombination, both factors leading to increased photo-catalytic activity. The one-pot sol–gel method [102, 103] and evaporation-driven self-assembly in a furnace aerosol reactor have been used to prepare Cu–TiO_2–SiO_2 catalysts for photo-reduction of CO_2 to methane and CO. The catalyst-preparation technique adopted resulted in very high dispersion and effective synergy between the active phases, TiO_2 and Cu oxide, in the mesoporous silica matrix, thereby increasing the rate of photo catalytic reduction of CO_2 to CO and methane. As shown in Table 6, below, Ying Li et al. [102] observed a distinct synergetic effect between the components when Cu–TiO_2–SiO_2 prepared by the one-pot sol–gel method was used for CO_2 photoreduction. Whereas the nominal effects of dispersion of TiO_2 on SiO_2 (increase in CO formed from 8.1 to 22.7 μmol/g TiO_2/h) and Cu loading on TiO_2 (increase in CO formed from 8.1 to 11.8 μmol/g TiO_2/h and additional methane formation of 1.8 μmol/g TiO_2/h) could be observed separately, the synergistic effect in the composite catalyst was apparent from the significant increase in CO (60 μmol/g TiO_2/h) and methane formation (10 μmol/g TiO_2/h). Specific catalyst preparation techniques thus facilitate positive interaction between the components of the composite, leading to improved performance.

Journal : Small-ext 11164 | Dispatch : 26-10-2012 | Pages : 38
Article No. : 783 | LE | TYPESET
MS Code : | CP | DISK

Table 6 CO and CH_4 formation on Cu/TiO_2 dispersed on mesoporous silica catalysts—synergetic effect [103]

Catalyst	CO formation (μmol/g TiO_2/h)	CH_4 formation (μmol/g TiO_2/h)
TiO_2	8.1	–
TiO_2–SiO_2	22.7	–
4 % Cu/TiO_2	11.8	1.8
0.5 % Cu/TiO_2–SiO_2	60.0	10

Pioneering work performed by Anpo and co-workers on a dispersion of titania as isolated nano-sized and molecular sized particles on micro-porous zeolite and mesoporous silica matrices has demonstrated that the local structure (surface coordination, tetrahedral vs. octahedral) and electronic states undergo significant modifications, affecting photo catalytic activity. Such a strategy for preparation of dispersed active phases, as described in a recent review [108], would be highly useful for design of improved catalysts.

Several novel catalyst systems, for example Ni at $NiO/InTaO_4$ [109], NiO/Co_3O_4–$InNbO_4$ [110], niobates in different forms, $Pt/NaNb_3O_8$, HNb_3O_8 nano belts [111], Pt/HNb_3O_8 [112, 113], silica-pillared HNb_3O_8 [114], Ag loaded layered titanates, $ALa_4Ti_4O_{15}$ (A = Ca, Sr, Ba) [115], $CuGaO_2$, and $CuGa_{(1-x)}Fe_xO_2$ [116], with significant CO_2 reduction capabilities have been investigated. Pt/mesoporous ZnGe oxynitride [117], and heterojunction photocatalysts, for example $FeTiO_3/TiO_2$ [118], $CdS(Bi_2S_3)TiO_2$ [119], and mesoporous Ga_2O_3 are another set of promising catalysts that deserve further investigation. Other notable developments in this area are the preparation and characterization of novel hetero structures based on ZnO–Fe_2O_3 [120], mesoporous $TiO_{2-x}N_x$ with unique worm-hole type morphology [121], adoption of solution combustion methods, and investigation of synergistic effects of N and S co-doping on titania [122].

Given the fact that backward reaction of CO_2 reduction products reduce overall yield of hydrocarbons, efforts are in progress to devise a reactor system in which anode oxidation and cathode reductions are carried out in different compartments separated by a proton-conducting membrane [123]. In processes that use a sacrificial electron donor, methods have been developed for regeneration and recycling of the donor so that process efficiency could be improved [124, 125]. Kim et al. [126]. have observed improvement in photo catalytic reduction of CO_2 after use of a thin Nafion layer on Pd/TiO_2 catalyst. The Nafion layer is expected to promote local proton activity within the layer, stabilize intermediates during CO_2 reduction, and inhibit re-oxidation of the reduction products.

Future directions

photo catalytic reduction of carbon dioxide with water to fuels and/or chemicals (methane, methanol, etc.) is an emerging area of research toward use of abundant sunlight. Although the process has the potential to become a viable and sustainable

Journal : Small-ext 11164 | Dispatch : 26-10-2012 | Pages : 38
Article No. : 783 | LE | TYPESET
MS Code : | CP | DISK

source of energy as an alternative to fossil fuels, it has resulted in several difficult challenges to scientists and technologists which have yet to be tackled, namely:

- facilitating activation of two of the most thermodynamically stable molecules, CO_2 and H_2O;
- conversions achieved so far are extremely small, <1 %, occurring at very slow rate;
- catalysts tend to become deactivated very quickly;
- the CO_2 photoreduction process is highly complex, involving multi-electron transfer, and is non-selective, leading to a range of C_1–C_3 compounds—reaction pathways have not yet been established;
- design of catalysts consisting of photo-active phase and/or support and co-catalysts aided by metal ion and/or anion doping and light harvesting components and/or sensitizers, as a functionally integrated composite, is equally complex;
- ideal catalysts are expected to have maximum efficiency at absorption of solar energy and have requisite band energy-level characteristics to drive the redox reactions;
- the process involves two steps, splitting of water and reduction of carbon dioxide, which is thermodynamically more favorable; because the second step involves multi-electron transfer, rates are very slow compared with the first step; these two steps must be synchronized to achieve higher yields of hydrocarbons;
- multiple and complex surface reaction pathways that involve several carbon-containing ion radicals, render the selective formation of methane or methanol a difficult task;
- further decomposition of the products and promotion of backward reactions also contribute to lower yields;
- catalyst deactivation proceeds through formation of carbonaceous species on the surface, implying that the metal function responsible for the hydrogenation of carbonaceous species must be improved, although availability of hydrogen via water splitting may not be an issue;
- although the primary objectives behind the wide range of modifications of the form of titania, namely promoting visible light activity, retarding the recombination of charge carriers by effective physical separation (by doping with metals, anions and cations), facilitating their transport through the titania surface, isolation of titania sites by dispersion on high-surface-area supports, and incorporation of suitable active elements to achieve the required redox reactions, have been realized to a significant extent, the expected improvement in activity has been moderate, a two or fourfold increase, which is too low for any possible practical applications; and
- in-depth investigation of surface reaction pathways by in-situ spectroscopic methods, supported by sound theoretical studies on the activation and surface transformations of CO_2 and other aspects of the investigation, as detailed in a previous section, would be helpful in controlling deactivation and achieving higher conversion.

Journal : Small-ext 11164 | Dispatch : 26-10-2012 | Pages : 38
Article No. : 783 | LE | TYPESET
MS Code : | CP | DISK

Nevertheless, research efforts on these topics are being pursued with the objectives of designing efficient catalyst systems to achieve higher yields of the desired products and improving catalyst life.

Efforts in the future must be toward the development of alternative catalysts, based on different semiconducting metal oxides/sulfides/nitrides/phosphides, layered titanates, and binary and ternary oxides of Nb, Ta, Ga, and In, in conjunction with alkaline, alkaline earth, and rare earth oxides and with a host of co-catalysts and sensitizers [1, 3, 7, 8, 18–22, 40, 97, 123, 127–129].

The following areas/aspects, especially, are worth further exploration.

- Several binary and ternary oxides of Bi, V, Nb, and Ta with group IIIA elements, for example Al, Ga, and In, are known to be efficient catalysts for photo catalytic splitting of water in the visible region [130, 131]. These systems with suitable co-catalysts, for example NiO could be excellent catalysts for CO_2 photoreduction.
- Most of these oxides are synthesized by high-temperature solid-state reaction with very low surface area. Soft chemistry routes could be investigated to obtain high-surface-area samples. However, in such cases, the contribution of residual carbon on the catalysts must be taken into account.
- These compounds have well-defined crystal structure and hence their solid state and photo-physical properties could be fine-tuned to derive maximum performance.
- Performance of such photocatalysts could be improved further by forming composites with advanced materials, for example CNT [83], graphene [132], and Nafion [126] which facilitate free and rapid transfer of charge carriers could be another way to improve performance.
- Studies should be conducted on modes of adsorption and activation of CO_2 on metals and metal oxides which act as co-catalysts—experimental and theoretical approaches should be pursued.
- Use of different co-catalysts, and single and bi-component systems, should be investigated.
- The mechanistic pathways of transformation of transient surface species and formation of C_2 and higher carbon-number products should be elucidated.
- Modes of deactivation of catalysts and possibilities of regeneration should be investigated.

It is expected that use of photoelectrochemical cells for conversion of CO_2 to methanol [133–135] would add another dimension to the process, furnishing improved yields of hydrocarbons. Development of novel and more efficient catalyst systems and prevention of re-oxidation of products could also help to improve the efficiency of the process.

Acknowledgments The authors gratefully acknowledge the Department of Science and Technology, Government of India, for the grant toward establishing NCCR at IIT, Madras, and M/s Hindustan Petroleum Corporation Limited, Mumbai, for a funding the project on photo-catalytic conversion of CO_2.

Journal : Small-ext 11164 | Dispatch : 26-10-2012 | Pages : 38
Article No. : 783 | LE | TYPESET
MS Code : | CP | DISK

References

1. L. Palmisano, A. Sclafani, in *Heterogeneous Photo Catalysis*, ed. by M. Schiavello (Wiley, Chichester), p. 109 (1997)
2. K. Demeestere, J. Dewulf, H.V. Langenhove, Crit. Rev. Environ. Sci. Technol. **37**, 489 (2007)
3. K. Kočí, L. Obalová, Z. Lacný, Chem. Pap. **62**, 1 (2008)
4. A. Fujishima, X. Zhang, T.A. Tryk, Int. J. Hydrog. Energy **32**, 2664 (2007)
5. M.R. Hoffmann, S.T. Martin, W. Choi, W. Detlef, Chem. Rev. **95**, 69 (1995)
6. L. Stroyuk, A.I. Kryukov, S.Y. Kuchmii, V.D. Pokhodenko, Theor. Exp. Chem. **45**, 209 (2009)
7. P. Ji, M. Takeuchi, T-M. Cuong, J. Zhang, M. Matsuoka, M. Anpo, Res. Chem. Intermed. **36**, 327 (2010)
8. Y. Yang, H. Zhong, C. Tian, Res. Chem. Intermed. **37**, 91 (2011)
9. H. Huang, X. Gub, J. Zhou, K. Ji, H. Liu, Y. Feng, Catal. Commun. **11**, 58 (2009)
10. J. Premkumar, R. Ramaraj, J. Photochem. Photobiol. A **110**, 53 (1997)
11. Z. Zhihuan, F. Jimin, W. Zhizhong, J. Clean. Prod. **15**, 1894 (2007)
12. L. Shaohua, Z. Zhihuan, W. Zhizhong, Photochem. Photobiol. Sci. **6**, 695 (2007)
13. L. Huang, F. Peng, H. Wang, H. Yu, Z. Li, Catal. Commun. **10**, 1839 (2009)
14. B.R. Hyun, Y.W. Zhong, A.C. Bartnik, L. Sun, H.D. Abruna, F.W. Wise, J.D. Goodreau, J.R. Matthews, T.M. Leslie, N.F. Borrelli, ACS Nano **2**, 2206 (2008)
15. C. Wang, K.W. Kwon, M.L. Odlyzko, B.H. Lee, M. Shim, J. Phys. Chem. C **111**, 11734 (2007)
16. C. Wong, R.L. Thompson, J. Baltrus, C. Matranga, J. Phys. Chem. Lett. **1**, 48 (2010)
17. A. Zaleska, Recent Pat. Eng. **2**, 157 (2008)
18. A. Fujishima, X. Zhang, D.A. Tryk, Surf. Sci. Rep. **63**, 515 (2008)
19. M. Anpo, M. Takeuchi, J. Catal. **216**, 505 (2003)
20. O. Ishitani, C. Inoue, Y. Suzuki, T. Ibusuki, J. Photochem. Photobiol. A **72**, 269 (1993)
21. M.A. Malati, W.K. Wong, Surf. Technol. **22**, 305 (1984)
22. P. Usubharatana, D. McMartin, A. Veawab, P. Tontiwachwuthikul, Ind. Eng. Chem. Res. **45**, 2558 (2006)
23. W. Choi, A. Termin, M.R. Hoffmann, J. Phys. Chem. **98**, 13669 (1994)
24. J.C. Colmenares, M.A. Aramendía, A. Marinas, J.M. Marinas, F.J. Urbano, J. Appl. Catal. A **306**, 120 (2006)
25. M. Bellardita, M. Addamo, A. Di Paola, L. Palmisano, Chem. Phys. **339**, 94 (2007)
26. J. Sá, M. Fernández-García, J.A. Anderson, Catal. Commun. **9**, 1991 (2008)
27. U.G. Akpan, B.H. Hameed, Appl. Catal. A **375**, 1 (2010)
28. R. Asahi, T. Morikawa, T. Ohwaki, K. Aoki, Y. Taga, Science **293**, 269 (2001)
29. T. Morikawa, R. Asahi, T. Ohwaki, A. Aoki, Y. Taga, Jpn. J. Appl. Phys. **20**, L-561 (2001)
30. C.D. Valentin, G. Pacchioni, A. Selloni, S. Livraghi, E. Giamello, J. Phys. Chem. B **109**, 11414 (2005)
31. C.D. Valentin, E. Finazzi, G. Pacchioni, A. Selloni, S. Livraghi, M.C. Paganini, E. Giamello, Chem. Phys. **339**, 44 (2007)
32. T.L. Diwald, T. Thompson, E.G. Zubkovc, S.D. Goralski, S.D. Walck, J.T. Yates, J. Phys. Chem. B **108**, 52 (2003)
33. T.L. Diwald, E.G. Thompson, S.D. Goralski, J.T. Walck, J. Yates, J. Phys. Chem. B **108**, 6004 (2004)
34. X. Chen, C. Burda, J. Phys. Chem. B **108**, 15446 (2004)
35. C.S. Gopinath, J. Phys. Chem. B **110**, 7079 (2006)
36. M. Satish, B. Viswanathan, R.P. Viswanath, C.S. Gopinath, Chem. Mater. **17**, 6349 (2005)
37. E.J. Maginn, J. Phys. Chem. Lett. **1**, 3478 (2010)
38. M.A. Scibioh, B. Viswanathan, Proc. Indian Natl Sci. Acad. **70A**, 407 (2004)
39. S.S. Nam, H. Kim, G. Kishan, M.J. Choi, K.W. Lee, Appl. Catal. A **179**, 155 (1999)
40. V.P. Indrakanti, J.D. Kubicki, H.H. Schobert, Energy Environ. Sci. **2**, 745 (2009)
41. T. Inoue, T.M. Fujishima, S. Konishi, K. Honda, Nature **277**, 637 (1979)
42. R.W. Matthews, S.R. McEvoy, J. Photochem. Photobiol. A **66**, 355 (1992)
43. J. Fan, E.Z. Liu, L. Tian, X.-Y. Hu, Q. He, T. Sun, J. Environ. Eng. **137**, 171 (2011)
44. Y. Liu, B. Huang, Y. Dai, X. Zhang, X. Qin, M. Jiang, M. Whangbo, Catal. Commun. **11**, 210 (2009)
45. T. Mizuno, K. Adachi, K. Ohta, A. Saji, J. Photochem. Photobiol. A **98**, 87 (1996)

Journal : Small-ext 11164 | Dispatch : 26-10-2012 | Pages : 38
Article No. : 783 | LE | TYPESET
MS Code : | CP | DISK

46. H. Hori, K. Koike, Y. Suzuki, M. Ishizuka, J. Tanaka, K. Takeuchi, Y. Sasaki, J. Mol. Catal. A **179**, 1 (2002)
47. S. Kaneco, H. Kurimoto, K. Ohta, T. Mizuno, S. Akira, J. Photochem. Photobiol. A **109**, 59 (1997)
48. S. Kaneco, H. Kurimoto, Y. Shimizu, K. Ohta, T. Mizuno, Energy **24**, 21 (1999)
49. S.S. Tan, L. Zou, E. Hu, Catal. Today **115**, 269–273 (2006)
50. S.S. Tan, L. Zou, E. Hu, Sci. Technol. Adv. Mater. **8**, 89 (2007)
51. K. Kočí, L. Obalová, L. Matějová, D. Plachá, Z. Lacný, J. Jirkovský, O. Šolcová, Appl. Catal. B **89**, 494 (2009)
52. K. Kočí, M. Reli, O. Kozák, Z. Lacný, D. Plachá, P. Praus, L. Obalová, Catal. Today **176**, 212 (2011)
53. T.-V. Nguyen, J.C.S. Wu, C.-H. Chiou, Catal. Commun. **9**, 2073–2076 (2008)
54. Y. Ku, W.-H. Lee, W.-Y. Wang, J. Mol. Catal. A **212**, 191 (2004)
55. K. Sayama, H. Arakawa, J. Chem. Soc. Faraday Trans. **93**, 1647 (1997)
56. I.H. Tseng, W.C. Chang, J.C.S. Wu, Appl. Catal. B **37**, 37 (2002)
57. B.J. Liu, T. Torimoto, H. Yoneyama, J. Photochem. Photobiol. A **113**, 93 (1998)
58. B.J. Liu, T. Torimoto, H. Matsumoto, H. Yoneyama, J. Photochem. Photobiol. A **108**, 187 (1997)
59. S. Kaneco, Y. Shimizu, K. Ohta, T. Mizuno, J. Photochem. Photobiol. A **115**, 223 (1998)
60. G.R. Dey, J. Nat. Gas Chem. **16**, 217 (2007)
61. G.R. Dey, A.D. Belapurkar, K. Kishore, J. Photochem. Photobiol. A **163**, 503 (2004)
62. M. Halmann, M. Ulman, B.A. Blajeni, Sol. Energy **31**, 429 (1983)
63. M. Halmann, V. Katzir, E. Borgarello, E. Kiwi, J. Sol. Energy Mater. **10**, 85 (1984)
64. M. Anpo, H. Yamashita, Y. Ichihashi, S. Ehara, J. Electroanal. Chem. **396**, 21–26 (1995)
65. M. Anpo, K. Chiba, J. Mol. Catal. **74**, 207 (1992)
66. K. Adachi, T. Mijuma, Sol. Energy **53**, 187 (1994)
67. Slamet, H.W. Nasution, E. Purnama, S. Kosela, J. Gunlazuardi, Catal. Commun. **6**, 313 (2005)
68. M. Varghese, O.K. Paulose, T.J. Latempa, Nano Lett. **9**, 731 (2009)
69. Q.H. Zhang, W.D. Han, Y.J. Hong, J.G. Yu, Catal. Today **148**, 335 (2009)
70. N. Sasirekha, S.J.S. Basha, K. Shanthi, Appl. Catal. B **62**, 169 (2006)
71. Y. Kohno, H. Hayashi, S. Takenaka, T. Tanaka, T. Funabiki, S. Yoshida, J. Photochem. Photobiol. A **126**, 117 (1999)
72. K. Koci, K. Mateju, L. Obalova, S. Krejcikova, Z. Lacny, D. Placha, L. Capek, A. Hospodkova, O. Solcova, Appl. Catal. B **96**, 239 (2010)
73. D. Luo, Y. Bi, W. Kan, N. Zhang, S. Hong, J. Mol. Struct. (2011). doi:10.1016/j.molstruc.2011.03.044
74. G. Guan, T. Kida, T. Harada, M. Isayama, A. Yoshida, Appl. Catal. A **249**, 11 (2003)
75. G. Guan, T. Kida, T. Ma, K. Kimura, E. Abe, A. Yoshida, Green Chem. **5**, 630–634 (2003)
76. G. Guan, T. Kida, A. Yoshida, Appl. Catal. B **41**, 387 (2003)
77. N. Ulagappan, H. Frei, J. Phys. Chem. A **104**, 7834 (2000)
78. W. Lin, H. Han, H. Frei, J. Phys. Chem. B **108**, 18269 (2004)
79. M. Anpo, H. Yamashita, Y. Ichihashi, Y. Fujii, M. Honda, J. Phys. Chem. B **101**, 2632 (1998)
80. M. Anpo, M. Takeuchi, J. Catal. **216**, 505 (2003) and references 125 to 140 therein
81. M. Anpo, H. Yamashita, K. Ikeue, Yu. Fuji, S.G. Zhang, Y. Ichihashi, D.R. Park, Y. Suzuki, K. Keilko, T. Tatsumi, Catal. Today **44**, 327 (1998)
82. Z. Zhao, J. Fan, M. Xie, Z. Wang, J. Clean. Prod. **17**, 1025 (2009)
83. X.-H. Xia, Z.-J. Jia, Y. Yu, Y. Liang, Z. Wang, L.-L. Ma, Carbon **45**, 717 (2007)
84. K. Rajalakshmi, V. Jeyalakshmi, K.R. Krishnamurthy, B. Viswanathan, Indian J. Chem. **51A**, 411 (2012)
85. C.C. Lo, C.H. Hung, C.S. Yuan, J.F. Wu, Sol. Energy Mater. Sol. Cells **91**, 1765 (2007)
86. H. Tsuneoka, K. Teramura, T. Shishido, T. Tanaka, J. Phys. Chem. C **114**, 8892 (2010)
87. K. Teramura, S. Okuoka, H. Tsuneoka, T. Shishido, T. Tanaka, Appl. Catal. B **96**, 565 (2010)
88. M. Watanabe, Surf. Sci. Lett. **279**, 236 (1992)
89. M. Kanemoto, T. Shiragami, C. Pac, S. Yanagida, J. Phys. Chem. C **96**, 3521 (1992)
90. Y. Wang, Y. Wang, Y. Gao, React. Kinet. Mech. Catal. **99**, 485 (2010)
91. N. Ahmed, Y. Shibata, T. Taniguchi, T. Izumi, J. Catal. (2011). doi:10.1016/j.jcat.2011.01.004
92. S.C. Yan, S.X. Ouyang, J. Gao, M. Yang, J.Y. Feng, X.X. Fan, L.J. Wan, Z.S. Li, J.H. Ye, Y. Zhou, Z.G. Zou, Angew. Chem. Int. Ed. **49**, 6400 (2010)
93. N.M. Dimitrijevic, B.K. Vijayan, O.G. Poluektov, T. Rajh, K.A. Gray, H. He, P. Zapol, J. Am. Chem. Soc. **133**, 3964 (2011)

Journal : **Small-ext 11164**	Dispatch : **26-10-2012**	Pages : **38**
Article No. : **783**	□ LE	□ TYPESET
MS Code :	☑ CP	☑ DISK

94. J.C.S. Wu, Catal. Surv. Asia **13**, 30 (2009)
95. J.C.S. Wu, C.W. Huang, Front. Chem. Eng. China **4**(2), 120 (2010)
96. M. Subrahmanyam, S. Kaneco, N. Alonso-Vante, Appl. Catal. B **23**, 169 (1999)
97. M.R. Hoffmann, J.A. Moss, M.M. Baum, Dalton Trans. **40**, 5151 (2011)
98. C.-C. Yang, J. Vernimmen, V. Meynen, P. Cool, G. Mul, J. Catal. **284**, 1 (2011)
99. C.-C. Yang, PhD Thesis, University of Twente, Twente, 2011
100. S.S. Tan, L. Zou, E. Hu, Catal. Today **131**, 125 (2008)
101. K. Koci, L. Obalova, O. Solcova, Chem. Process Eng. **31**, 395 (2010)
102. W. Wang, J. Park, P. Biswas, Catal. Sci. Technol. **1**, 593 (2011)
103. Y. Li, W. Wang, Z. Zhan, M. Woo, C. Wu, P. Biswas, Appl. Catal. B **100**, 386 (2010)
104. E. Fujita, Coord. Chem. Rev. **185–186**, 373 (1999)
105. I. Willner, R. Maidan, D. Mandler, H. Dum, G. Dorr, K. Zengerle, J. Am. Chem. Soc. **109**, 6080 (1987)
106. A.J. Morris, G.J. Meyer, E. Fujita, Acc. Chem. Res. **42**, 1983 (2009)
107. D.C. Grills, E. Fujita, J. Phys. Chem. Lett. **1**, 2709 (2010)
108. K. Mori, H. Yamashita, M. Anpo, RSC Adv. **2**, 3165 (2012)
109. C.W. Tsai, H.M. Chen, R.S. Liu, K. Asakura, T.S. Chan, J. Phys. Chem. C **115**, 10180 (2011)
110. D.S. Lee, H.J. Chen, Y.W. Chen, J. Phys. Chem. Solids **73**, 661 (2012)
111. X. Li, H. Pan, W. Li, Z. Zhuang, Appl. Catal. A **413–414**, 103 (2012)
112. H. Shi, T. Wang, J. Chen, C. Zhu, J. Ye, Catal. Lett. **141**, 525 (2011)
113. P. Li, S. Ouyang, G. Xi, T. Kako, J. Ye, J. Phys. Chem. C **116**, 7621 (2012)
114. X. Li, W. Li, Z. Zhuang, Y. Zhong, Q. Li, L. Wang, J. Phys. Chem. C (2012). doi: 10.1021/jp303365z
115. K. Iizuka, T. Wato, Y. Miseki, K. Saito, A. Kudo, J. Am. Chem. Soc. **133**, 20863 (2011)
116. J.W. Lekse, M.K. Underwood, J.P. Lewis, C. Matranga, J. Phys. Chem. C **116**, 1865 (2012)
117. N. Zhang, S. Ouyang, T. Kako, J. Ye, Chem. Commun. **48**, 1269 (2012)
118. Q.D. Truong, J.Y. Liu, C.C. Chung, Y.C. Ling, Catal. Commun. **19**, 85 (2012)
119. X. Li, H. Liu, D. Luo, J. Li, Y. Huang, Y. Fang, Y. Xu, L. Zhu, Chem. Eng. J. **180**, 151 (2012)
120. G.K. Pradhan, S. Martha, K.M. Parida, ACS Appl. Mater. Interfaces **4**, 707 (2012)
121. K. Sivaranjani, C.S. Gopinath, J. Mater. Chem. **21**, 2639 (2011)
122. B. Naik, K.M. Parida, C.S. Gopinath, J. Phys. Chem. C **114**, 19473 (2010)
123. Y. Izumi, Coord. Chem. Rev. (2012). http://dx.doi.org/10/.1016/j.ccr.2012.04.018. Accessed 13 April 2012
124. J. Michl, Nat. Chem. **3**, 268 (2011)
125. R.D. Richardson, E.J. Holland, B.K. Carpenter, Nat. Chem. **3**, 301 (2011)
126. W. Kim, T. Seok, W. Choi, Energy Environ. Sci. **5**, 6066 (2012)
127. Z. Jiang, T. Xiao, V.L. Kuznetsov, P.P. Edwards, Philos. Trans. R. Soc. A **368**, 3343 (2010)
128. K. Li, D. Martin, J. Tang, Chin. J. Catal. **32**, 879 (2011)
129. O.K. Varghese, M. Paulose, T.J. Latempa, C.A. Grimes, Nano Lett. **9**, 731 (2009)
130. W. Junhu, Z. Zhigang, Ye. Jinhua, J. Alloys Compd. **377**, 248 (2004)
131. J. Ye, Z. Zou, H. Arakawa, M. Oshikiri, M. Shimoda, A. Matsushita, T. Shishido, J. Photochem. Photobiol. A **148**, 79 (2002)
132. Y.T. Liang, B.K. Vijayan, K.A. Gray, M.C. Hersam, Nano Lett. **11**, 2865 (2011)
133. G. Seshadri, C. Lin, A.B. Bocarsly, J. Electroanal. Chem. **372**, 145 (1994)
134. I. Ganesh, Mater. Sci. Appl. **2**, 1407 (2011)
135. Y.R. Smith, V. Subramanian, B. Viswanathan, in *Photo-Electrochemistry and Photo Biology for Sustainability*, Chap. 9, eds. by S. Kaneco, B. Viswanathan, H. Katsumataby (Bentham Science, Sharjah, 2010), pp. 1217–1242

Journal : **Small-ext 11164** Dispatch : **26-10-2012** Pages : **38**
Article No. : **783** □ LE □ TYPESET
MS Code : ☑ CP ☑ DISK